

Recent Trends in Fluid Dynamics

Laszlo P. Csernai,
University of Bergen,
Norway



**International School "Relativistic Heavy Ion Collisions,
Cosmology and Dark Matter, Cancer Therapy" (15-26.05.2017)**

László Pál CSERNAI



Professor
Theoretical and Energy Physics Unit
[Teoretisk og energi fysikk gruppe]
Institute for Physics and Technology
University of Bergen
Room 512, Bjørn Trumpys hus
Allégt. 55, 5007 Bergen, Norway

Phone : +47 55 58 2802
Fax : +47 55 58 9440

<http://www.csernai.no/Csernai-textbook.pdf>

★ Enclosed please find more information on:

- **NEWS & GENERAL TOPICS**
- **RECENT TALKS**
- **Research and Teaching**
- **Curriculum Vitae** and List of Publications
- Degrees, honours, awards:
Prof., Dr., Dr.h.c., Dr.Sc., C.Sc., DNVA, MAE, EM-HAS, NTVA, FIAS, HM-HAE
- See also the textbook [Full Text] - **Introduction to Relativistic Heavy Ion Collisions** >
- **Németh László** (1901-1975) Hungarian writer



Last updated: Jan. 31, 2014, L.P. Csernai.

Introduction to Relativistic Heavy Ion Collisions

LÁSZLÓ P. CSERNAI

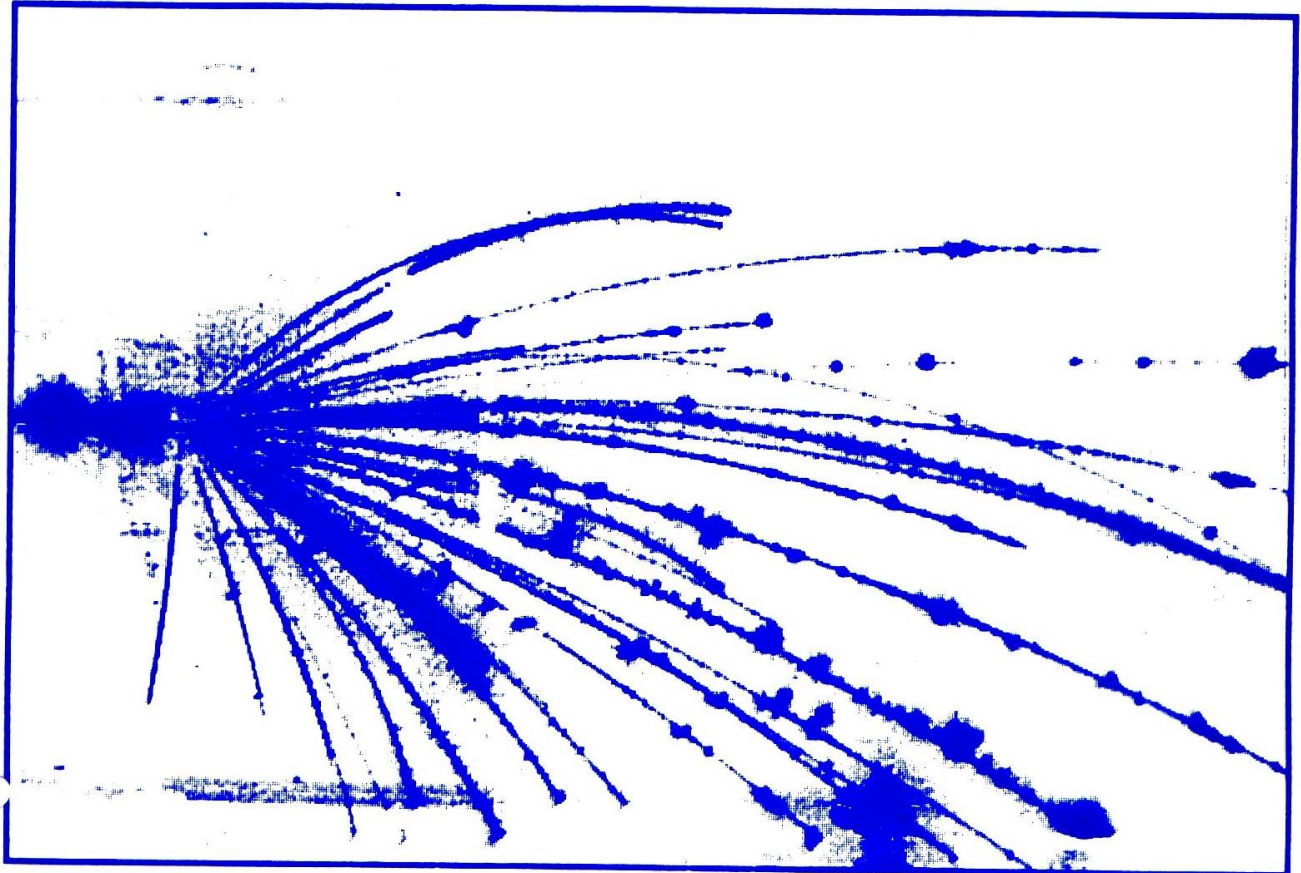
John Wiley and Sons Ltd,
Chicester, New York, Brisbane, Toronto, Singapore, 1994
ISBN - 0-471-93420-8

MULTIFRAGMENTATION (20+)

M-ch =
20 - 50

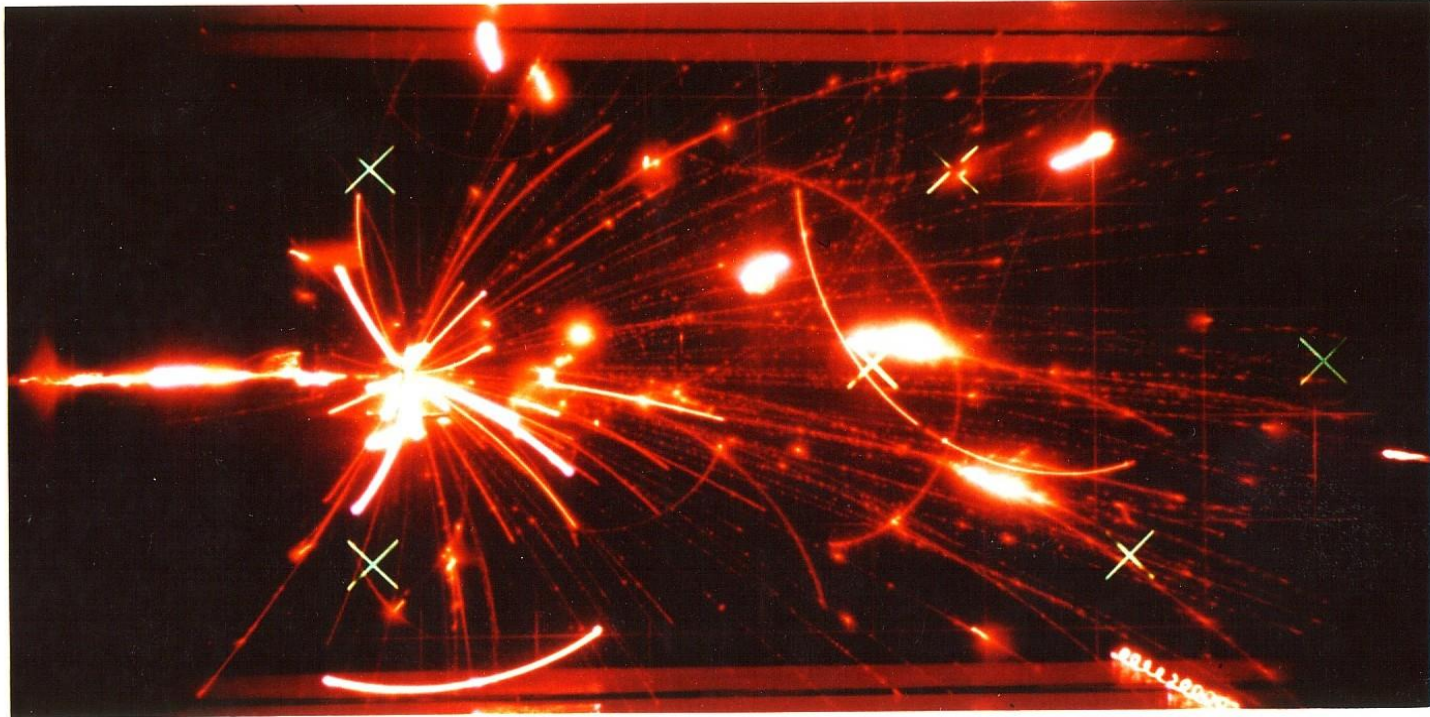
Positive
fragments

MSU CCD CAMERA SYSTEM



50 MeV/nucleon La+La CENTRAL TRIGGER
LBL STREAMER CHAMBER

RELATIVISTIC NUCLEAR COLLISION (1.8 A GeV Ar on Pb)



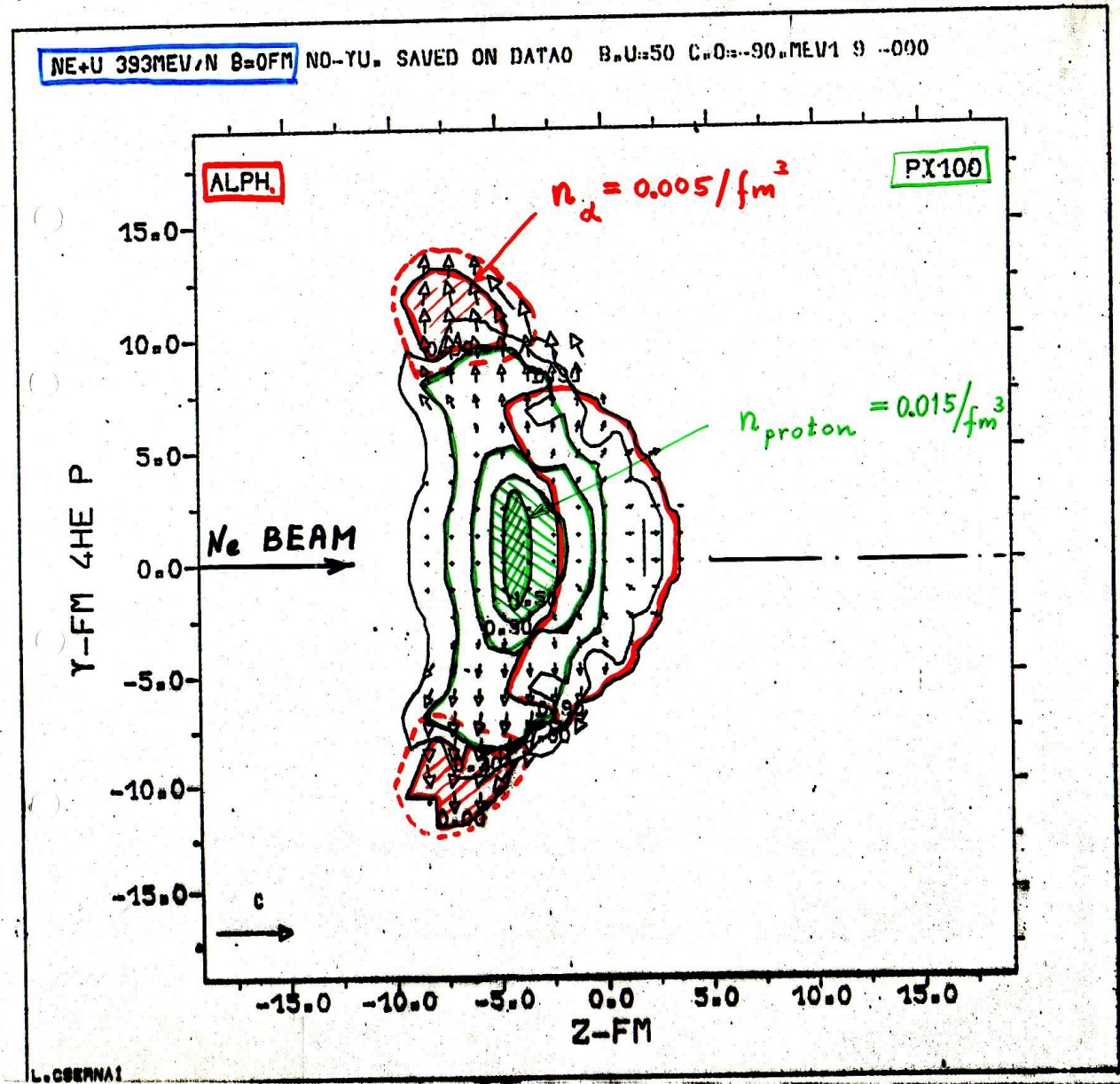
photographed by

UNIVERSITY of CALIFORNIA, RIVERSIDE
PHYSICS DEPARTMENT.

Central
shock
wave

Mach
cone

Fluid
dynamic
models
from
1980s



NE+U 393MEV/N B=5FM NO-YU. SAVED ON DATA5 BU=40 Cn0=-90nMEV1 9 -000
with Stöcker, Subramanian et al. PRC (1983)

Non-central
shock wave

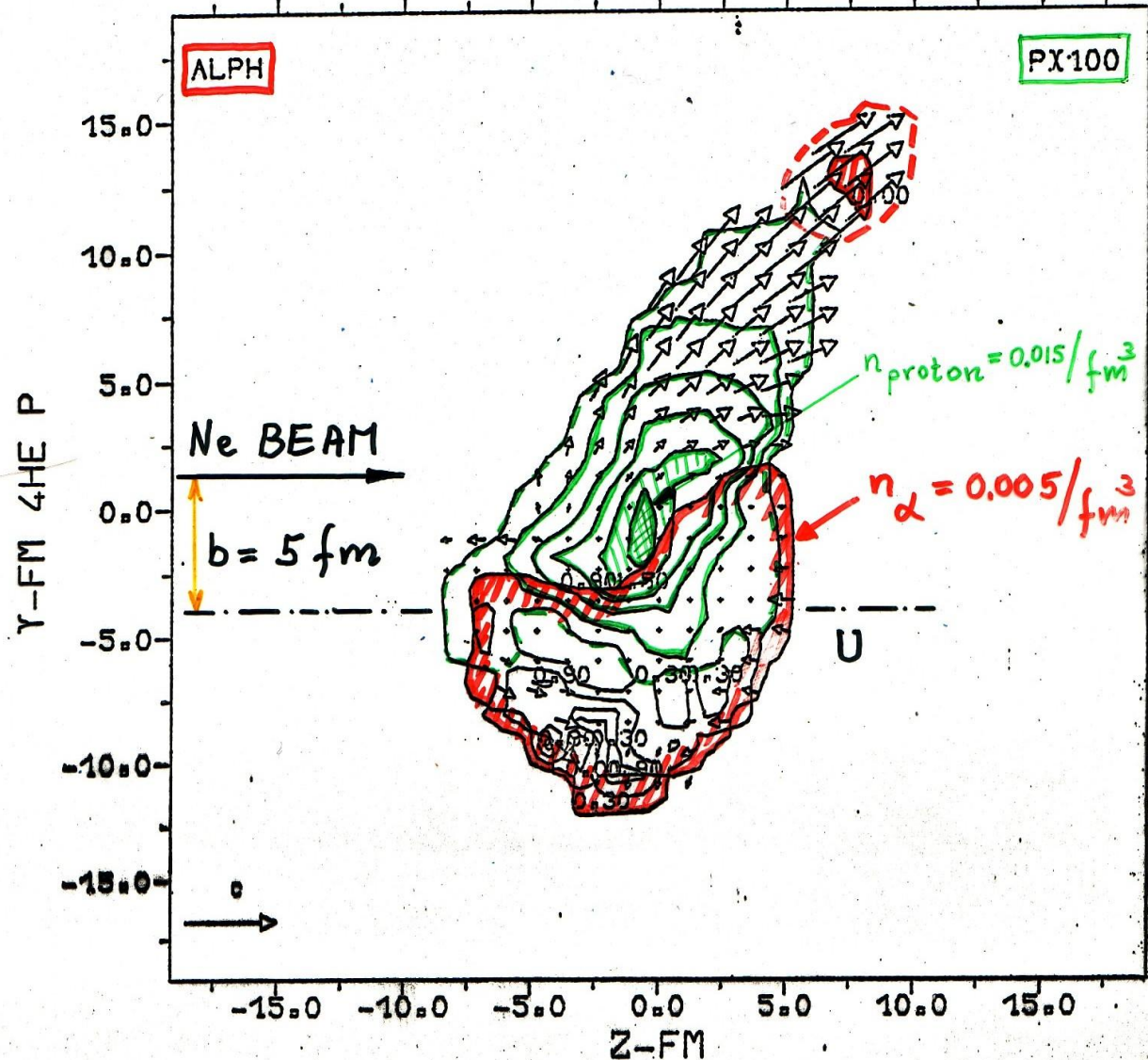
=>

Bounce-off

Side splash

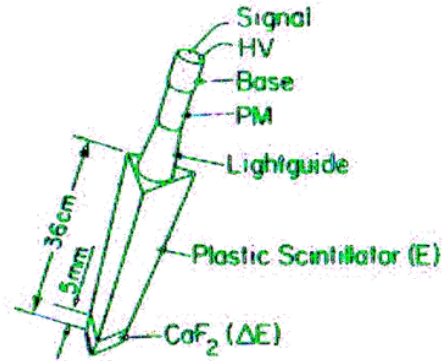
Directed
transverse
flow

Fluid
dynamic
models
from
1980s

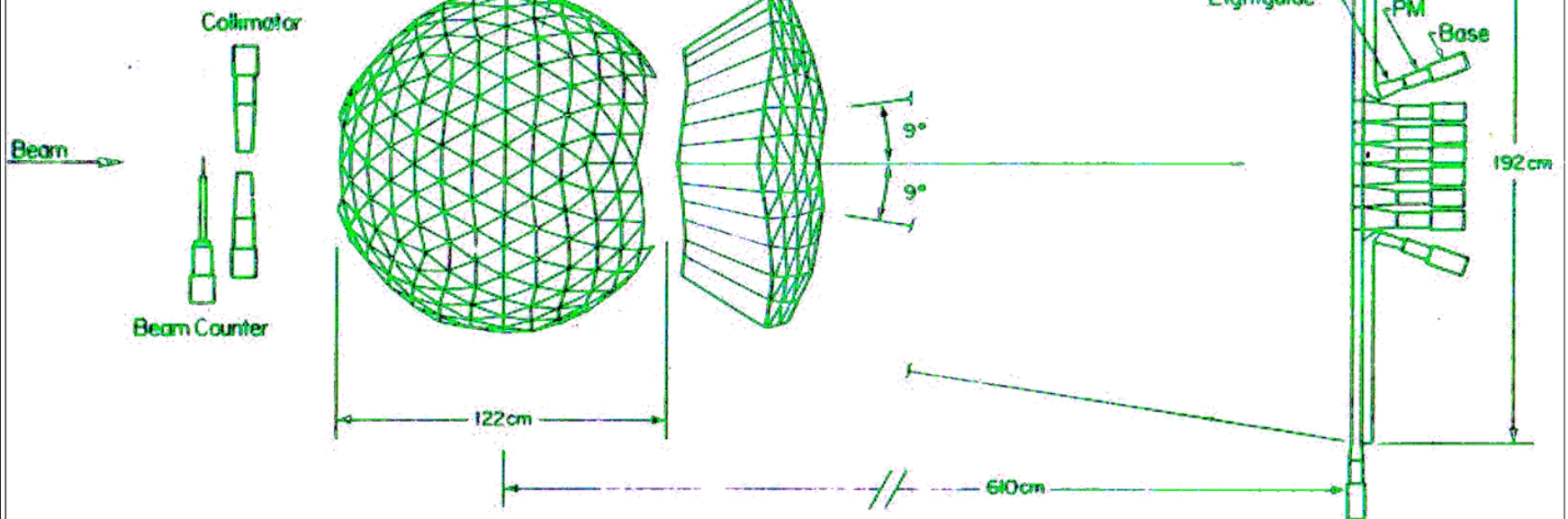
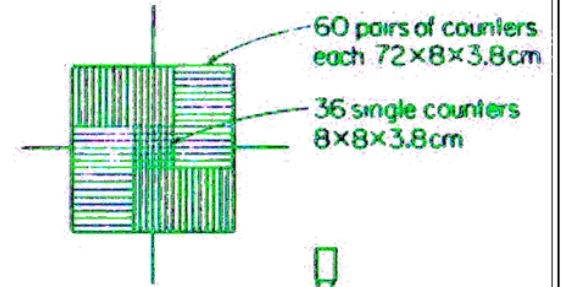


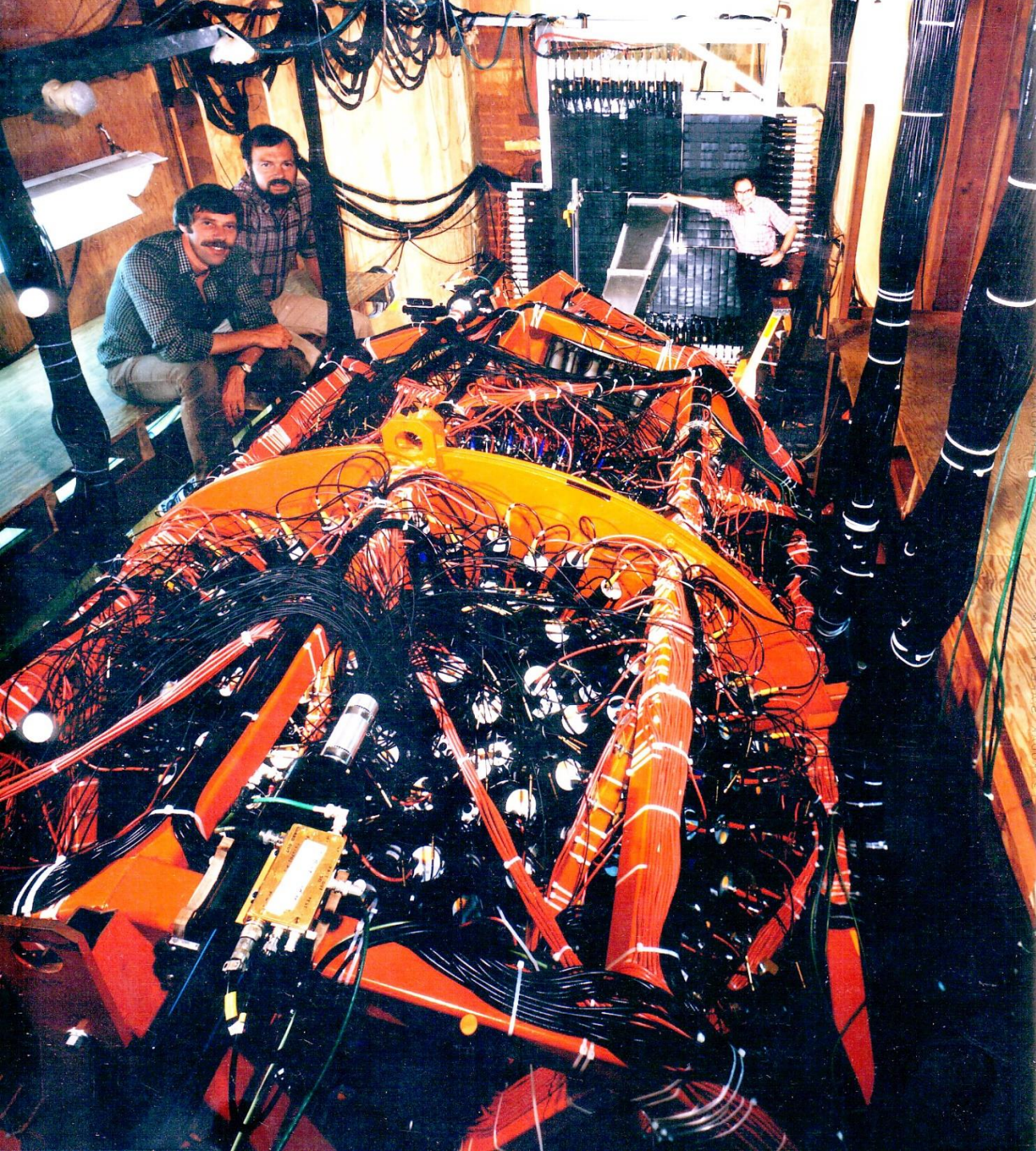
PLASTIC BALL

655 modules + 160



PLASTIC WALL





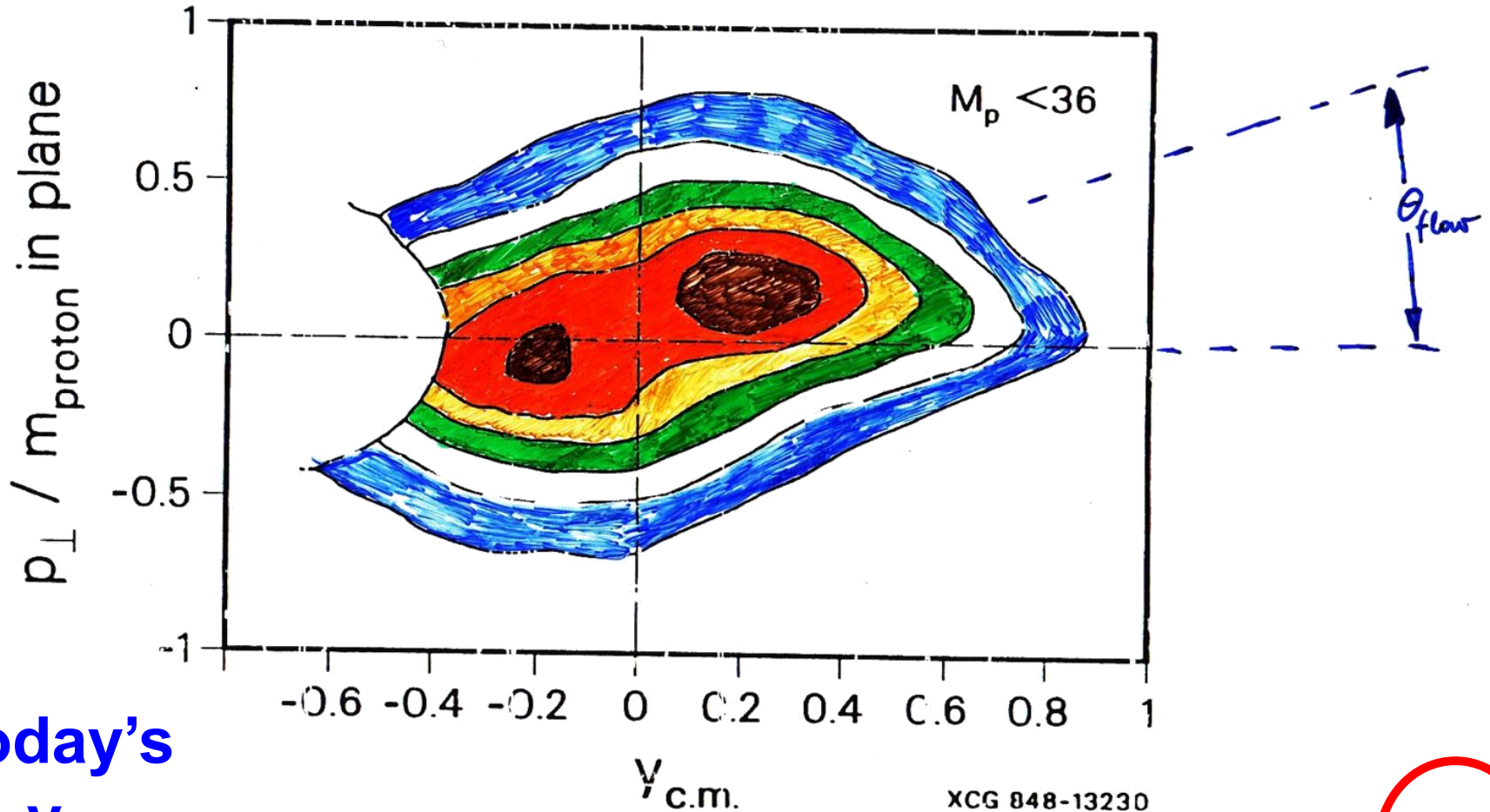
Plastic Ball & Wall

**Side-splash of
Bounce off
was observed
in the Plastic
Ball 1984**

**Made it to the
New York
Times!**

H.G. Ritter
H. Gutbrod
A. Poskanzer

$^{40}\text{Ar} + \text{Pb} ; 0.77 \text{ AGeV}$



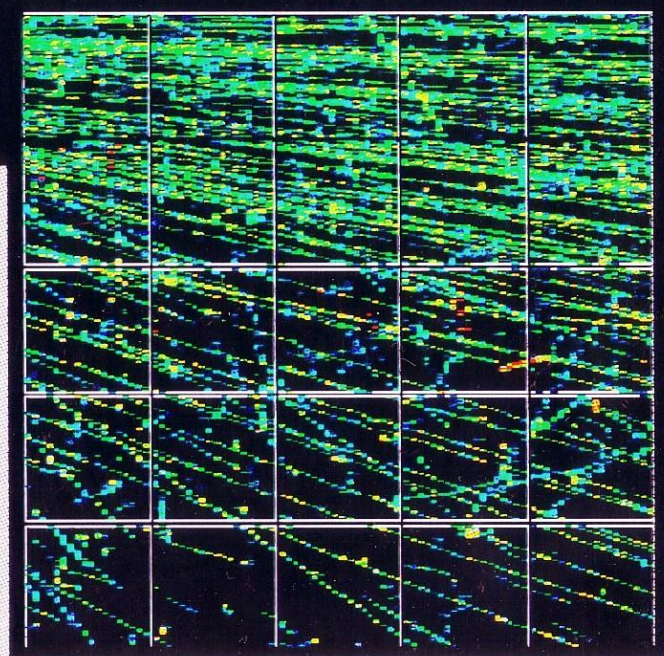
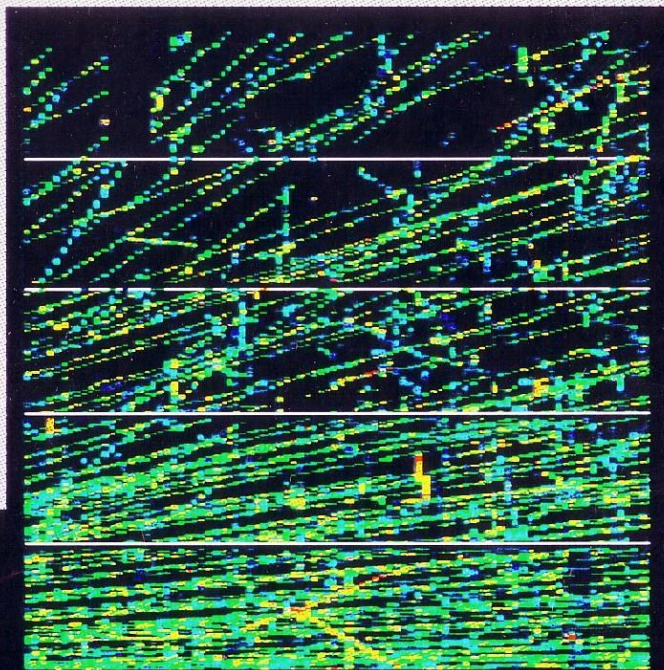
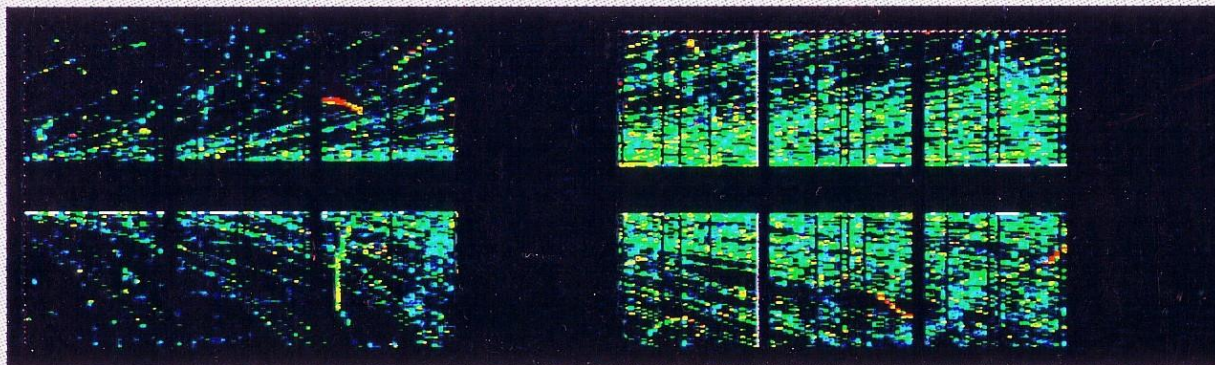
$M_p < 36$

Today's
 V_1

Figure 8

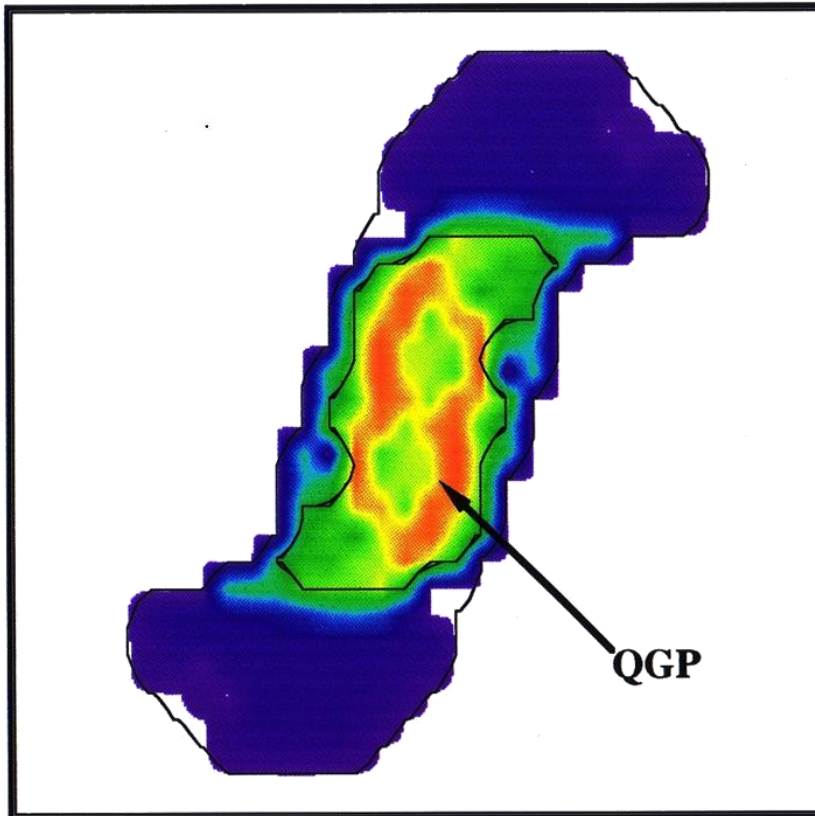
XCG 848-13230

H.G. Ritter, H. Gutbrod et al. 1985



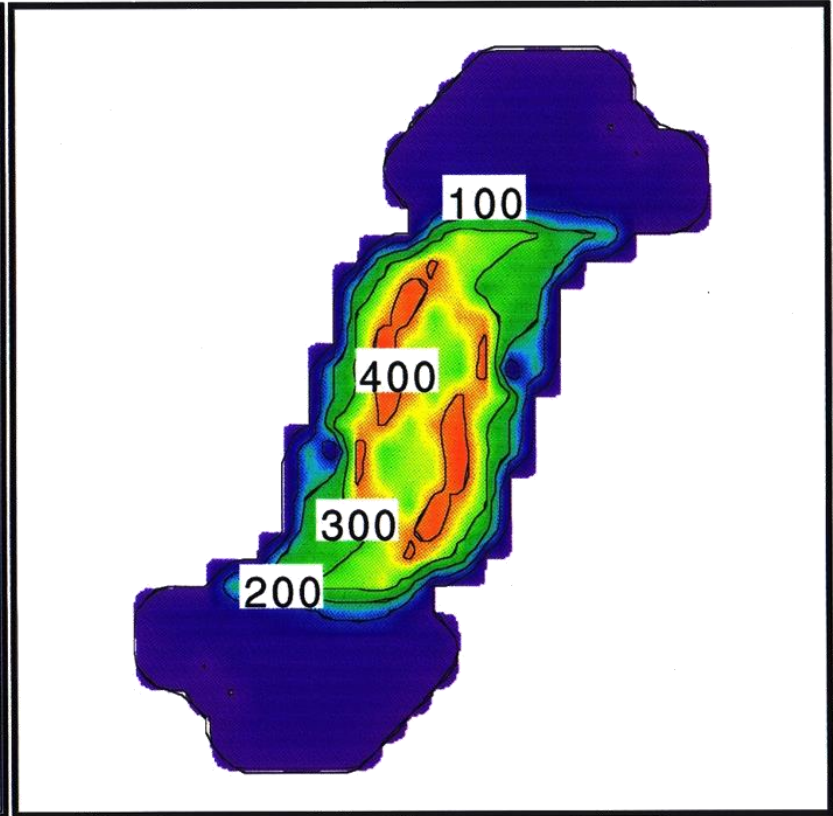
NA49 Pb-Pb 158 GeV/nucleon

Pb + Pb 160 GeV/u



One Fluid Hydro

Sierk-Nix + QGP
K=550



temperature

$1.37 \text{ fm}/c$

80's PIC Hydro model
results -> QGP

3. Relativistic Boltzmann Transport Equation

The relativistic Boltzmann Transport Equation (BTE) describes the time evolution of the single particle distribution function $f(x, p)$.

Based on the following assumptions:

- 1 Only two-particle collisions are considered, the so called binary collisions.
- 2 “Stoßzahlansatz” or assumption of “Molecular Chaos”: Number of binary collisions at x is proportional to $f(x, p_1) \times f(x, p_2)$.
- 3 $f(x, p)$ is a smoothly varying function compared to the mean free path (m.f.p.)

3.1 Particle conservation

Number of particles in a 3-dim. volume element at \vec{x} & time t , $\Delta N(x)$, is identical to the number of world-lines crossing a 3-dim. (time-like) hyper surface:

$$\Delta N(x) = \int_{\Delta^3\sigma} d^3\sigma_\mu N^\mu(x') = \int_{\Delta^3\sigma} \int_{\Delta^3p} d^3\sigma_\mu \frac{d^3p}{p^0} p^\mu f(x', p). \quad (3.1)$$



Number of particles scattering out of $\Delta^3p \Delta^4x$ is

$$\frac{1}{2} \Delta^4x \frac{\Delta^3p}{p^0} \int \frac{d^3p_1}{p_1^0} \frac{d^3p'}{p'^0} \frac{d^3p'_1}{p_1'^0} f(x, p) f(x, p_1) W(p, p_1 | p', p'_1). \quad (3.8)$$

The factor $\frac{1}{2}$: symmetry under the exchange $p, p_1 \leftrightarrow p'_1, p'$, and we correct for double counting. Similarly the change due to the gain term is:

$$\frac{1}{2} \Delta^4x \frac{\Delta^3p}{p^0} \int \frac{d^3p_1}{p_1^0} \frac{d^3p'}{p'^0} \frac{d^3p'_1}{p_1'^0} f(x, p') f(x, p'_1) W(p', p'_1 | p, p_1). \quad (3.9)$$

• Thus the total transport equation is:

$$p^\mu \partial_\mu f(x, p) = C(x, p), \quad (3.10)$$

where

$$C(x, p) = \frac{1}{2} \int \frac{d^3p_1}{p_1^0} \frac{d^3p'}{p'^0} \frac{d^3p'_1}{p_1'^0} [f' f'_1 W(p', p'_1 | p, p_1) - f f_1 W(p, p_1 | p', p'_1)], \quad (3.11)$$

and

$$f' \equiv f(x, p'), \quad f'_1 \equiv f(x, p'_1), \quad f \equiv f(x, p), \quad f_1 \equiv f(x, p_1). \quad (3.12)$$

3.6.1 Conservation of particle number

In this case $\Psi_k = 1$. Let us take the BTE

$$p_k^\mu f_{k,\mu} = \sum_{l=1}^N C_{kl}(x, p_k), \quad (3.46)$$

multiply it with Ψ_k , sum it over k and integrate it over $\int \frac{d^3 p_k}{p_k^0}$:

$$\sum_{k=1}^N \int \frac{d^3 p_k}{p_k^0} p_k^\mu f_{k,\mu} = \sum_{k,l=1}^N \int \frac{d^3 p_k}{p_k^0} C_{kl}(x, p_k). \quad (3.47)$$

Lemma \rightsquigarrow right hand side vanishes. Since the particle four current is $N^\mu = \int \frac{d^3 p_k}{p_k^0} p_k^\mu f_k$ equation (3.47) means that the 4 divergence of the particle current vanishes:

$$N^\mu{}_{,\mu} = \sum_{k=1}^N N_k^\mu{}_{,\mu} = 0. \quad (3.48)$$

- This is the Continuity Equation.

It expresses the fact that the particle number is conserved if it is conserved in a microscopic collision.

3.6.3 Conservation of energy and momentum

Choose $\Psi_k = p_k^\nu$. Let us take the BTE again

$$p_k^\mu f_{k,\mu} = \sum_{l=1}^N C_{kl}(x, p_k), \quad (3.51)$$

multiply it with Ψ_k , sum it over k and integrate it over $\int \frac{d^3 p_k}{p_k}$:

$$\sum_{k=1}^N \int \frac{d^3 p_k}{p_k^0} p_k^\mu p_k^\nu f_{k,\mu} = \sum_{k,l=1}^N \int \frac{d^3 p_k}{p_k^0} p_k^\nu C_{kl}(x, p_k). \quad (3.52)$$

Lemma \rightsquigarrow right hand side vanishes. Since the energy-momentum tensor is $T^{\mu\nu} = \int \frac{d^3 p_k}{p_k^0} p_k^\mu p_k^\nu f_k$, equation (3.52) means that the 4 divergence of the energy-momentum tensor vanishes:

$$T^{\mu\nu}{}_{,\mu} = \sum_{k=1}^N T_k^{\mu\nu}{}_{,\mu} = 0. \quad (3.53)$$

- This is the energy and momentum conservation. Equations (3.48-53) are also the equations of the *relativistic fluid dynamics*.

- In fluid dynamics these equations are postulated and not derived. As a matter of fact equations (3.48-53) are *not a closed set of equations*, because the energy-momentum tensor and the particle 4-current should be defined too.

In the transport theory this is done through the distribution function, which is known only if the solution of the BTE is known. Thus within the transport theory these equations do not provide us the solution of a dynamical problem.

3.7 Boltzmann H-theorem

The definition of the entropy 4-current in transport theory is

$$S^\mu = - \sum_k \int \frac{d^3 p_k}{p_k^0} p_k^\mu f_k [\log f_k - 1]. \quad (3.54)$$

($c = \hbar = k = 1$) The entropy should be a non-decreasing function of time, i.e. $S^\mu{}_{,\mu} \geq 0$.

We want to see if this is a consequence of the BTE or not.

Calculate the 4 divergence of the entropy current according to the definition

$$S^\mu{}_{,\mu} = - \sum_k \int \frac{d^3 p_k}{p_k^0} p_k^\mu [\log f_k] f_{k,\mu}. \quad (3.55)$$

From the Boltzmann Transport Equation $p_k^\mu f_{k,\mu} = \sum_l C_{kl}(x, p_k)$. Inserting this into the equation above

$$S^\mu{}_{,\mu} = - \sum_k \int \frac{d^3 p_k}{p_k^0} [\log f_k] C_{kl}(x, p_k). \quad (3.56)$$

Repeat the steps of the Lemma in the previous section, with $\Psi_k = \log f_k$.

$\log f_k$ is not a collision invariant: the integral will not necessarily vanish, but we still can get it into a symmetrized form by using the same steps:

$$S^\mu{}_{,\mu} = - \sum_{ijkl} \frac{1}{4} \int \frac{d^3 p_i}{p_i^0} \frac{d^3 p_j}{p_j^0} \frac{d^3 p_k}{p_k^0} \frac{d^3 p_l}{p_l^0} \left[\log \frac{f_k f_l}{f_i f_j} \right] f_i f_j W_{ij|kl}. \quad (3.57)$$

Summing up equations (3.57) and (3.60) we obtain:

$$S^{\mu, \mu} = \frac{1}{4} \sum_{ijkl} \int \frac{d^3 p_i}{p_i^0} \frac{d^3 p_j}{p_j^0} \frac{d^3 p_k}{p_k^0} \frac{d^3 p_l}{p_l^0} \left[\frac{f_k f_l}{f_i f_j} - \log \frac{f_k f_l}{f_i f_j} - 1 \right] f_i f_j W_{ij|kl}. \quad (3.61)$$

The expression in parentheses is a function, $g(x) = x - \log(x) - 1$, which is depicted in Figure 3.7.

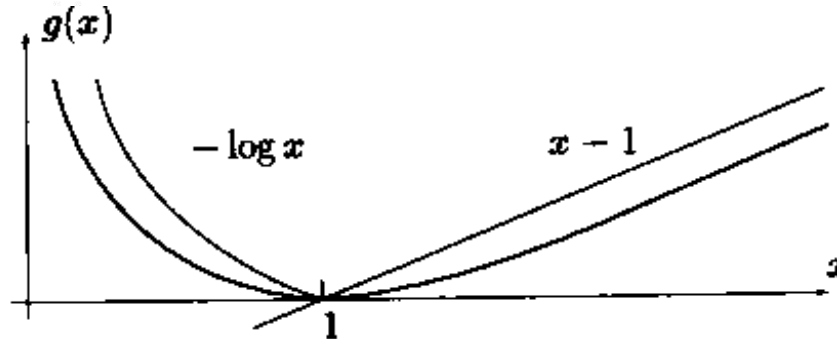


Figure 3.7 The $g(x) = x - \ln(x) - 1$ function

Since the distribution function is never negative, the argument of function $g(x)$ is also non-negative, thus it follows that $g(x) \geq 0$.

- The above equation then yields

$$S^{\mu, \mu} \geq 0, \quad (3.62)$$

and it vanishes only if $x = 1$, i.e. if $f_k f_l = f_i f_j$.

= stationary solution
→ Equilibrium $f(x,p)$

3.9 Zeroth order approximation

Perfect fluid dynamics

ASSUMPTIONS:

- (1) Our system is not homogeneous, but the gradients are small, so local distributions can be written as

$$f(x, p) = \frac{1}{(2\pi\hbar)^3} \exp\left(\frac{\mu_{ch}(x) - p^\mu u_\mu(x)}{T(x)}\right), \quad (3.70)$$

- (2) Local $n(x), P(x), e(x), s(x)$ are also known (from $f(x, p)$ by using the definitions)
- (3) We assume (!) that in the (LR), $T^{\mu\nu}$ is diagonal. (This is also a consequence of assumption (1), since we have neglected the gradients of the flow velocity and of the thermodynamical variables:

$$T_{LR}^{\mu\nu} = T_{LR}^{\mu\nu (0)} = (e + P)u_{LR}^\mu u_{LR}^\nu - P g^{\mu\nu} = \begin{pmatrix} e & 0 & 0 & 0 \\ 0 & P & 0 & 0 \\ 0 & 0 & P & 0 \\ 0 & 0 & 0 & P \end{pmatrix}_{LR} \quad (3.71)$$

The equations of **Perfect Fluid Dynamics** are the conservation laws under the assumption that $f(x, p) = f^{Juttner}(x, p)$

$$N^\mu{}_{,\mu} = 0 \quad \text{or} \quad \partial_\mu(nu^\mu) = 0, \quad (3.72)$$

and

$$T^\mu{}_{,\mu} = 0 \quad \text{or} \quad \partial_\mu(T^{\mu\nu}) = 0. \quad (3.73)$$

5.2 Perfect fluid dynamics

- Chapter 3: Conservation laws of a continuum can be expressed in a differential form via the energy-momentum tensor \sim FD.

- Validity of equations is wider!

- Dense liquids can also be described by these equations.

The equations of Perfect Fluid Dynamics are the conservation laws

$$N^{\mu}_{,\mu} = 0 \quad \text{or} \quad \partial_{\mu}(nw^{\mu}) = 0, \quad (5.1)$$

and

$$T^{\mu\nu}_{,\mu} = 0 \quad \text{or} \quad \partial_{\mu}(T^{\mu\nu}) = 0. \quad (5.2)$$

Using $w^{\mu} = (\gamma, \gamma\mathbf{v})$, $w = e + P$, $T^{ik} = w\gamma^2 v_i v_k + P\delta_{ik}$, $T^{0i} = -T_{0i} = w\gamma^2 v_i$, $T^{00} = T_{00} = (e + Pv^2)\gamma^2$, and introducing the apparent density

$$\mathcal{N} \equiv n\gamma = \mathbf{n}, \quad (5.3)$$

and the momentum current density and apparent energy density:

$$\mathcal{M} \equiv T^{0i} = w\gamma^2 \mathbf{v}, \quad (5.4)$$

$$\mathcal{E} \equiv T^{00} = (e + P\mathbf{v}^2)\gamma^2, \quad (5.5)$$

the equations of fluid dynamics take the more familiar form.

The continuity equation

$$(\partial_t + \mathbf{v} \text{ grad})\mathcal{N} = -\mathcal{N} \text{ div} \mathbf{v}. \quad (5.6)$$

The energy and momentum conservation will take the form

$$(\partial_t + \mathbf{v} \text{ grad})\mathcal{M} = -\mathcal{M}(\text{div} \mathbf{v}) - \text{grad} P, \quad (5.7)$$

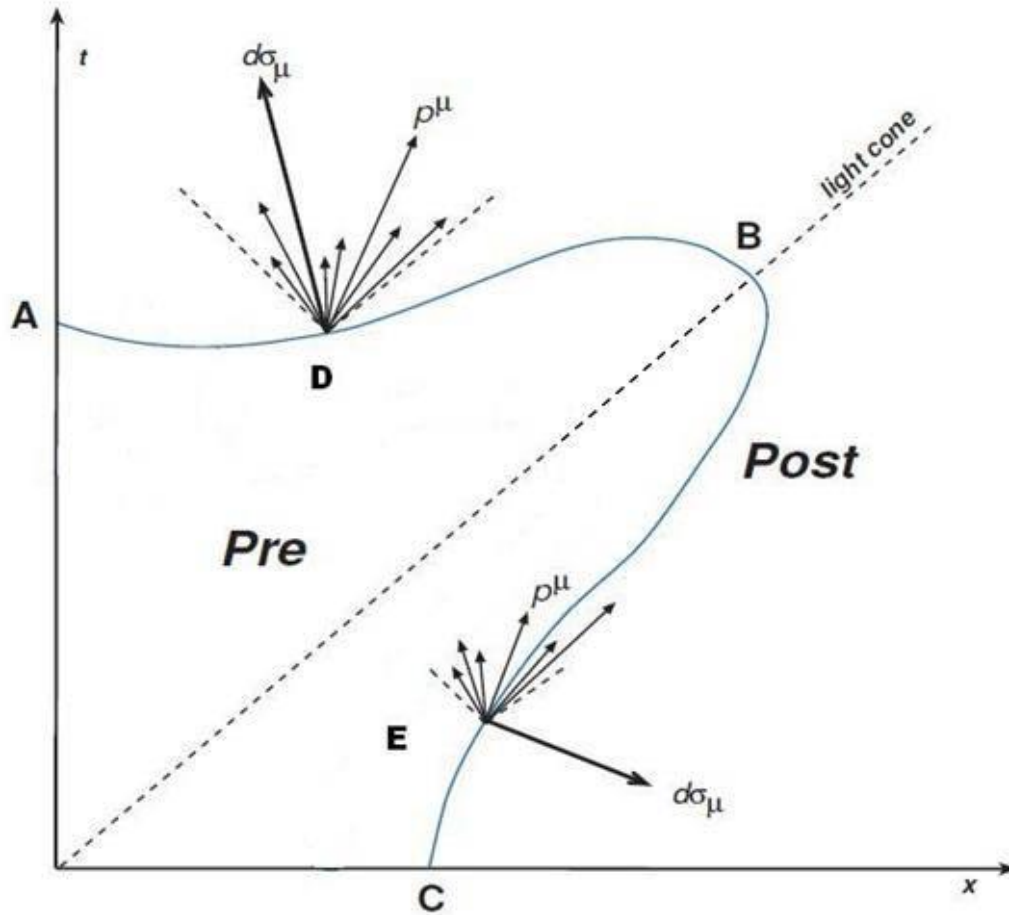
$$(\partial_t + \mathbf{v} \text{ grad})\mathcal{E} = -\mathcal{E} \text{ div} \mathbf{v} - \text{div}(P \mathbf{v}). \quad (5.8)$$

- Last two equations: Euler equation of fluid dynamics, and energy conservation.
- \mathcal{N} , \mathcal{E} , \mathcal{M} not directly from EOS, but solve algebraic equations (5.3-5), to obtain the thermodynamical quantities.
- Equations of fluid dynamics are not complete without an EOS.
- Viscous fluid dynamics is seldom used in relativistic physics.

Due to the fact that there are still questions around the proper relativistic generalization of viscous fluid dynamics [10]. It was shown that the usual relativistic generalizations of viscous fluid dynamics may lead to unstable solutions. Dissipative effects are, nevertheless, important as many non-relativistic calculations indicate. There exist a few relativistic viscous calculations which can be viewed upon as approximations.

Then let's repeat the conservation laws!

Discontinuities: IS, FO (CF), Shocks, Detonations



$$[N^\mu d\sigma_\mu] = 0;$$

$$[T^{\mu\nu} d\sigma_\mu] = 0;$$

$$[S^\mu d\sigma_\mu] \geq 0,$$

with

$$j = N^\mu d\sigma_\mu$$

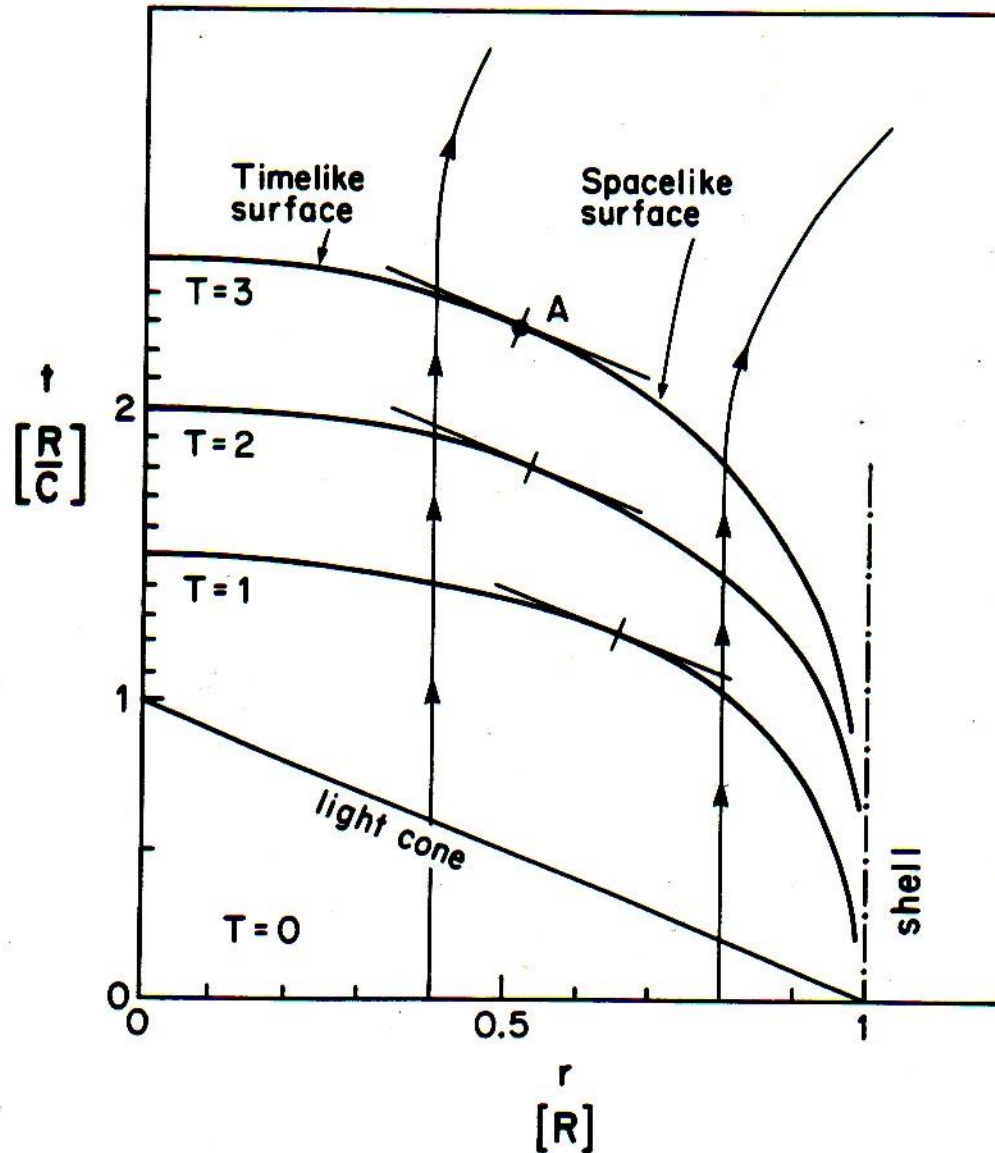
$$A^\mu = T^{\mu\nu} d\sigma_\nu$$

**Valid for non
Eq. also !!!**

Radiation dominated implosion



Timelike Detonation



Relativistic discontinuities

Can be space-like or time-like !!!

→ Cooling and expansion \approx

FO

→ Heating iwards, implosion

Aside: Taub-adiabat and Rayleigh line

Comparing the two equations for the current, j , :

$$\frac{[P](\Lambda^\mu \Lambda_\mu)}{[X]} = \frac{[wX]}{[X^2](\Lambda^\mu \Lambda_\mu)} \quad \rightsquigarrow \quad \frac{[P](\Lambda^\mu \Lambda_\mu)^2}{[X]} = \frac{[wX]}{[X](X_2 + X_1)},$$

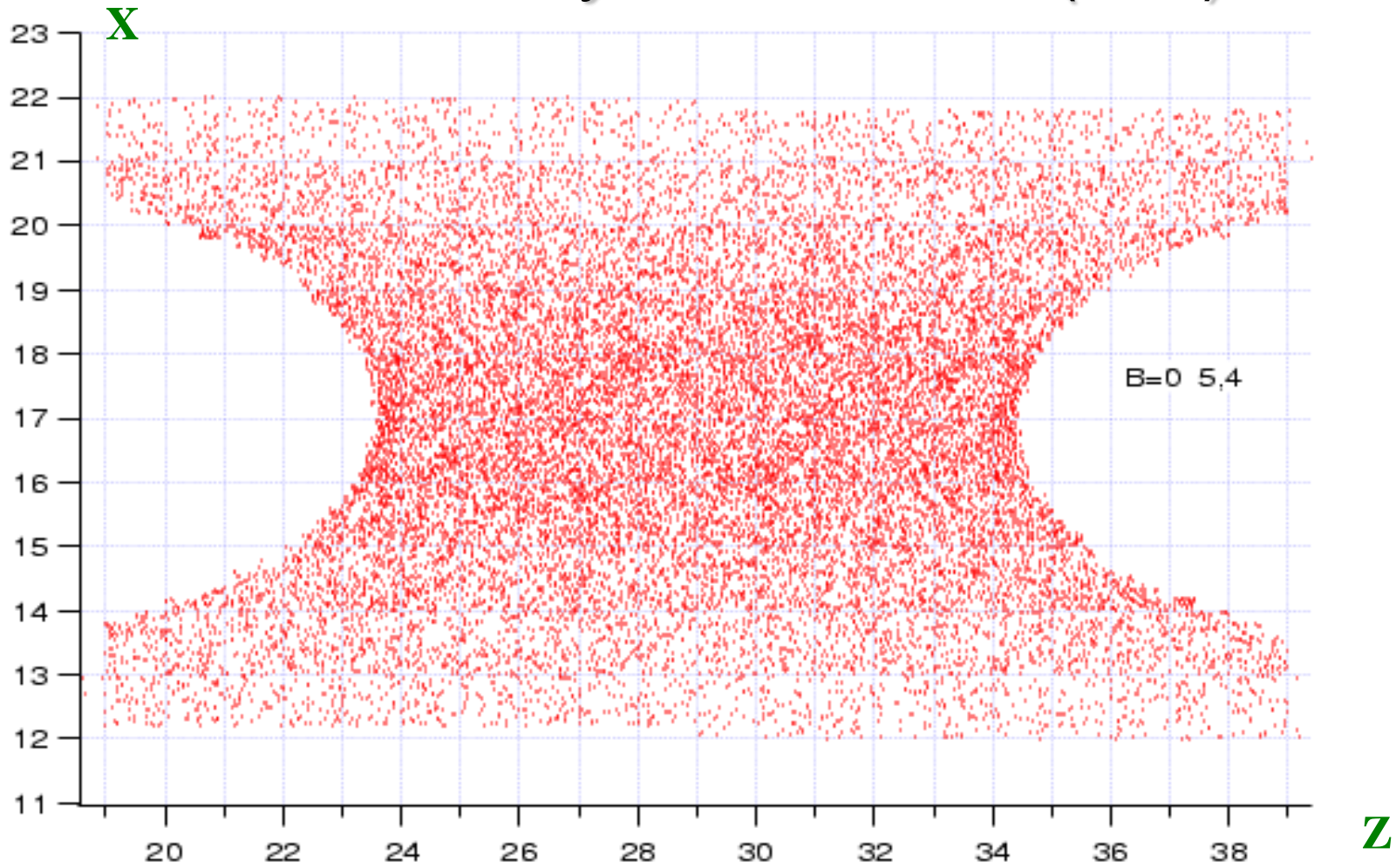
So, we obtain the **Taub adiabat** :

$$[P] = \frac{[wX]}{(X_2 + X_1)}.$$

The locus of the possible final states, “2”, lies on the Taub adiabat. If the initial state and the EoS of the final state is known the Taub adiabat with the Rayleigh line determine the final state.

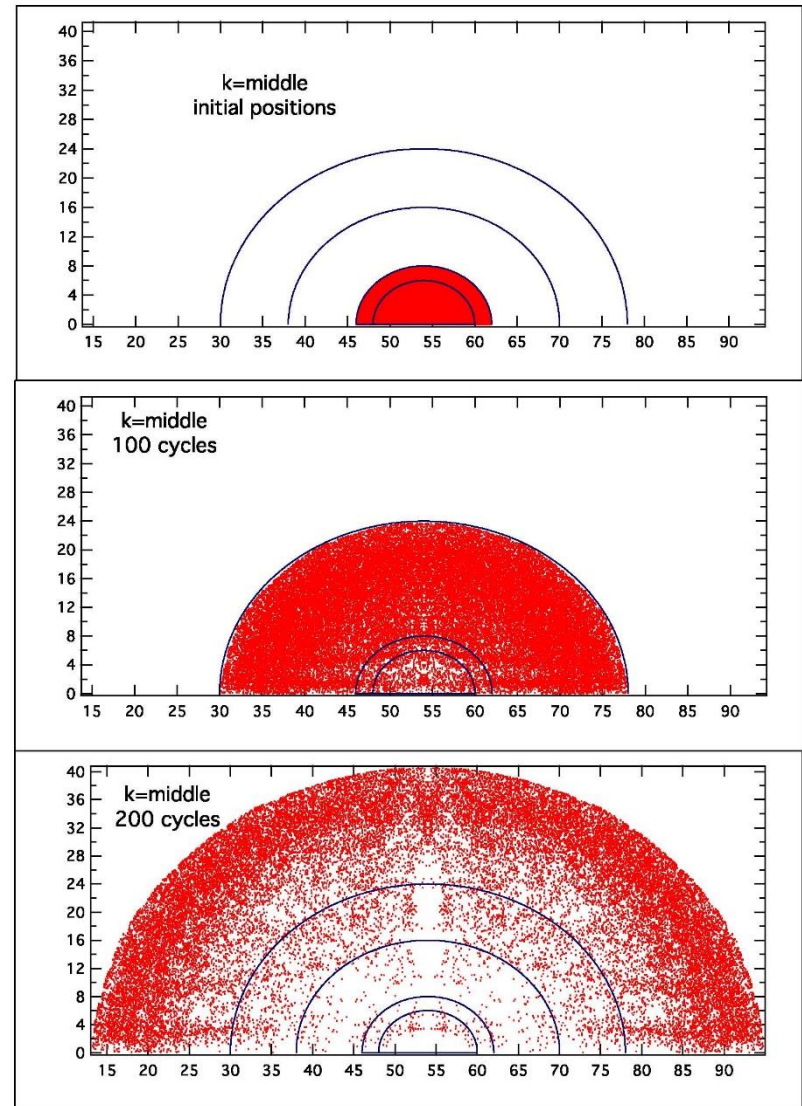
If the final state is **out of equilibrium**, I.e. not a perfect fluid, **this is not applicable!**

3-Dim Hydro for RHIC (PIC)

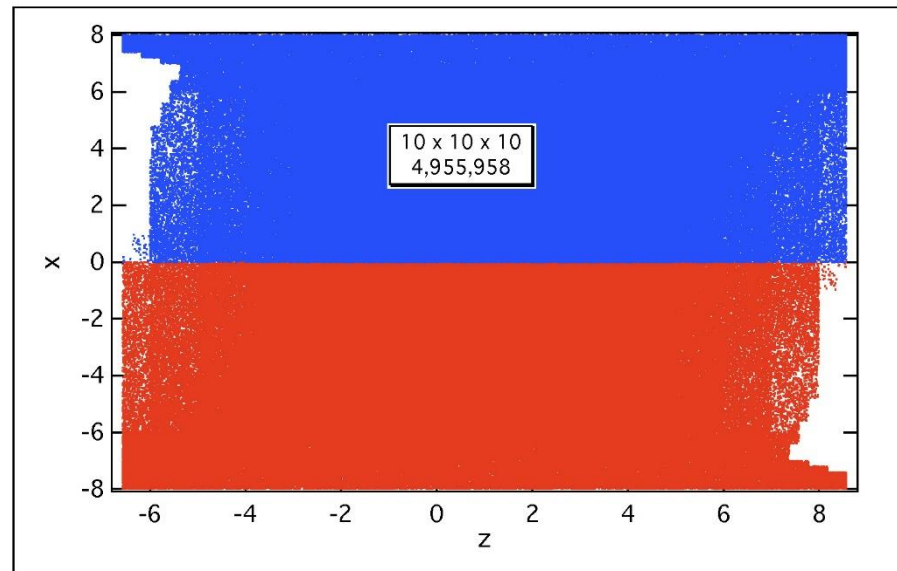
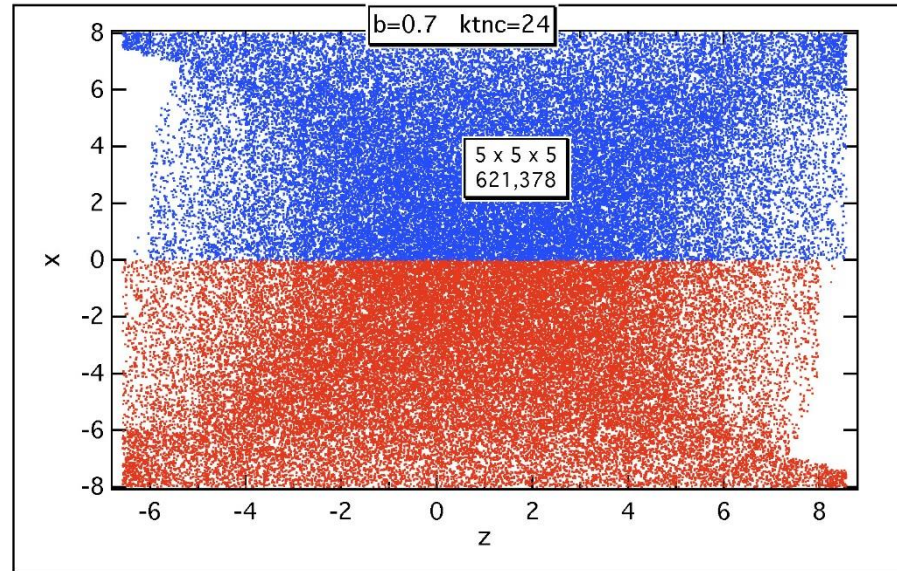


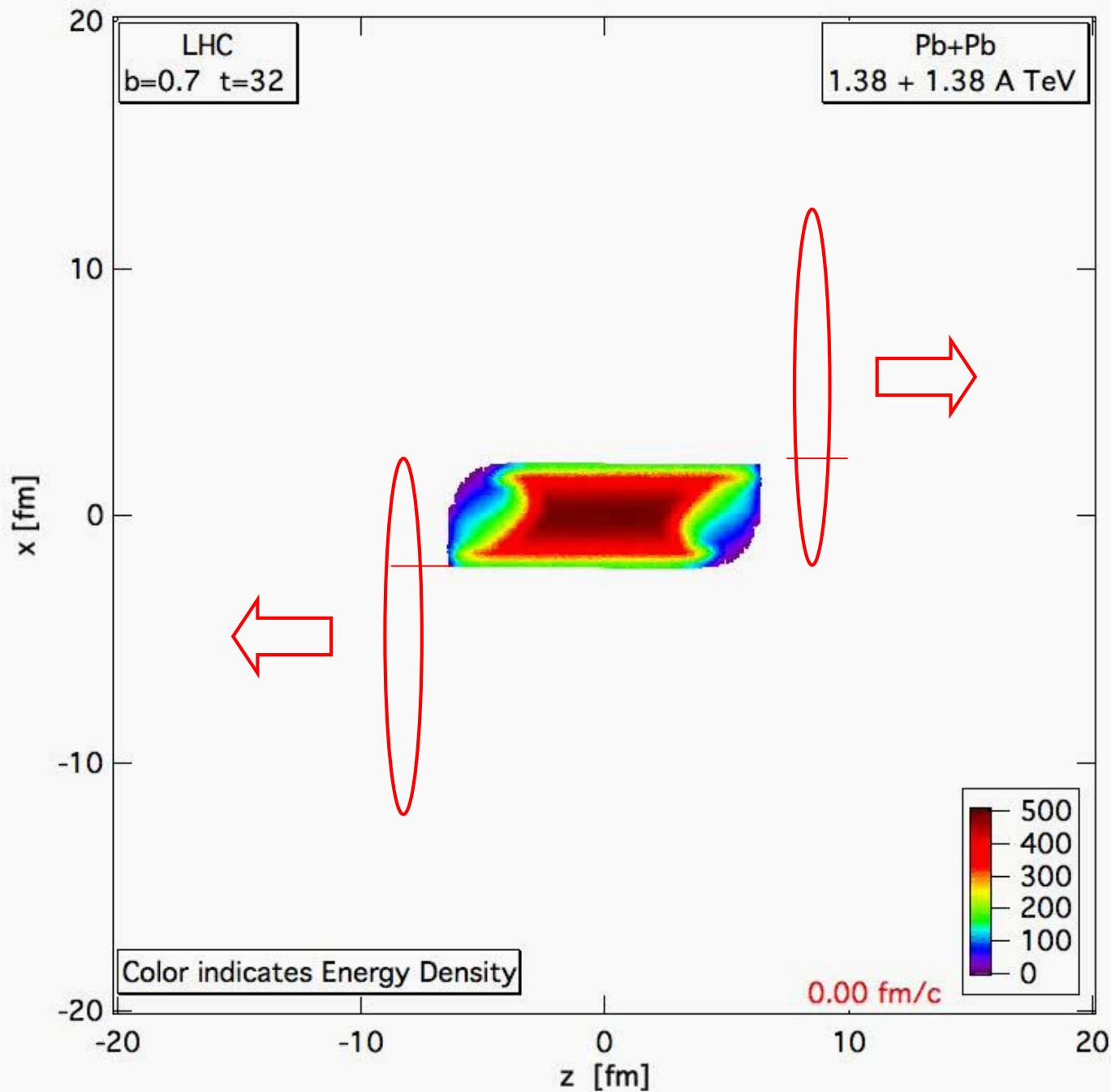
Test: Symmetric Expansion

- Code is written in Cartesian coordinates
- Starting with a cylindrically symmetric state -> expansion should be symmetric
- Figure shows a slice through the centre of the matter
- Expansion remains symmetric well beyond the limits of the validity of fluid dynamics despite using a cubic grid



Varying the Number of Markers





PIC- hydro

Pb+Pb 1.38+1.38 A TeV,
b= 70 % of b_max

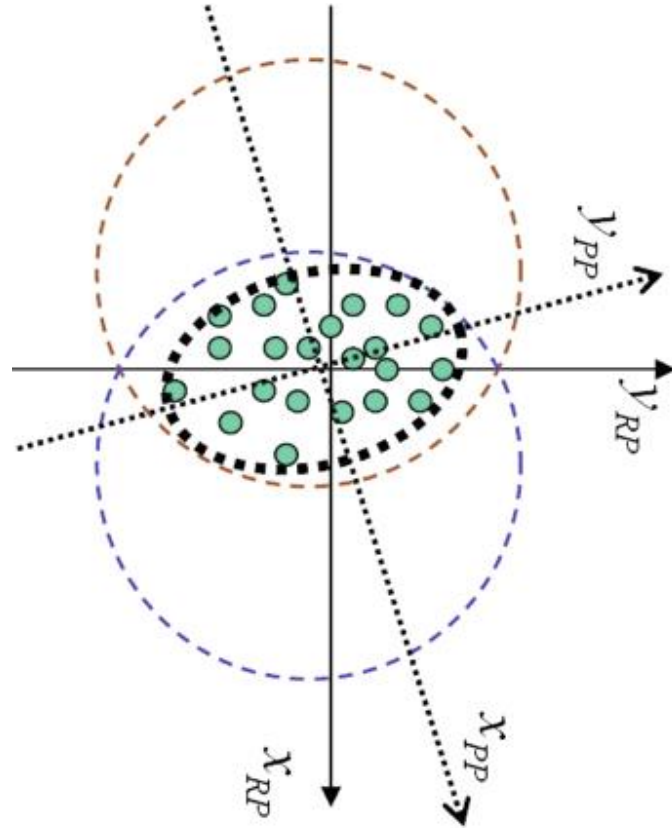
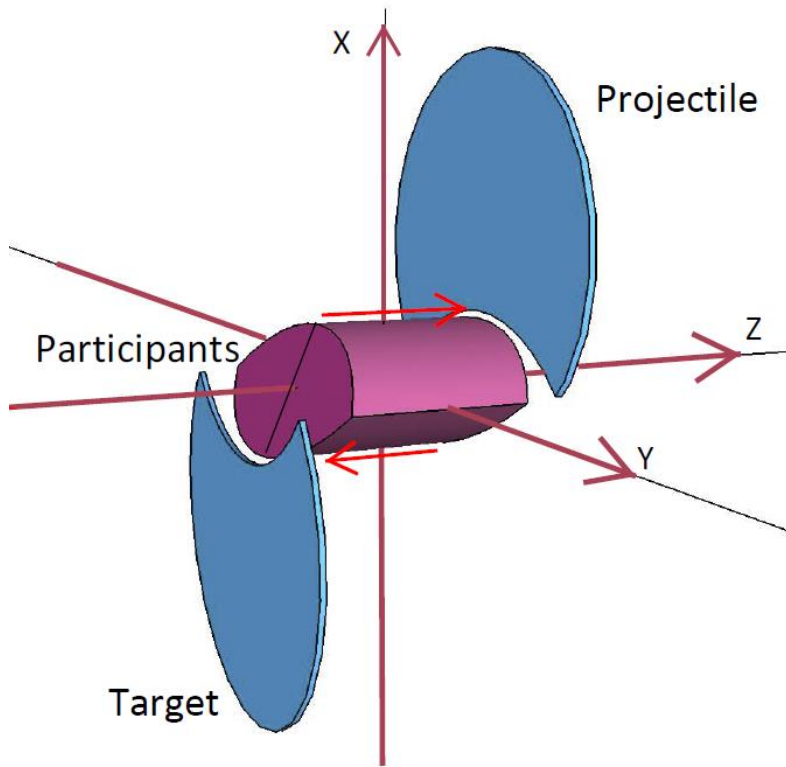
Lagrangian fluid cells,
moving, ~ 5 mill.

MIT Bag m. EoS

FO at $T \sim 200$ MeV, but
calculated much longer,
until pressure is zero
for 90% of the cells.

Structure and
asymmetries of init.
state are maintained in
nearly perfect
expansion.

Peripheral Collisions (A+A) → v_2 flow



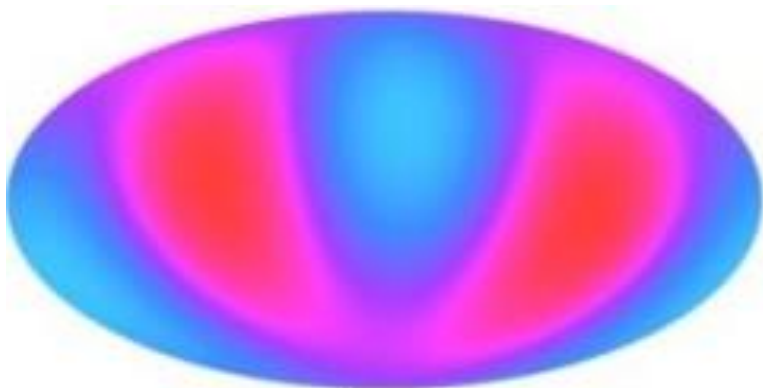
$$\frac{d^3 N}{dy dp_t d\phi} = \frac{1}{2\pi} \frac{d^2 N}{dy dp_t} [1 + 2v_1(y, p_t) \cos(\phi) + \underline{2v_2(y, p_t) \cos(2\phi)} + \dots]$$

Fluctuating Initial States in Central Heavy Ion Collisions

- 1980s $p_{x/m}$ directed flow
- 1990s v_1, v_2, \dots
- 2000... v_n and fluctuations in $[x,y]$ plane
→ transport properties, viscosity
- 2010 Longitudinal fluctuations ?
- 2015 L_y , rotation, turbulence, polarization

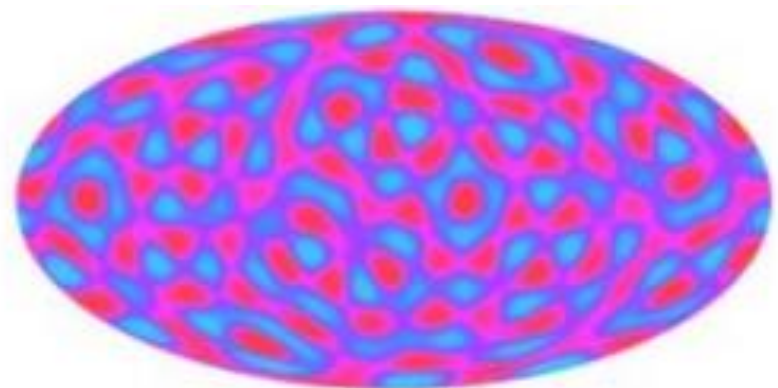
In Central Heavy Ion Collisions

~ like Elliptic flow, v_2



$l = 2$

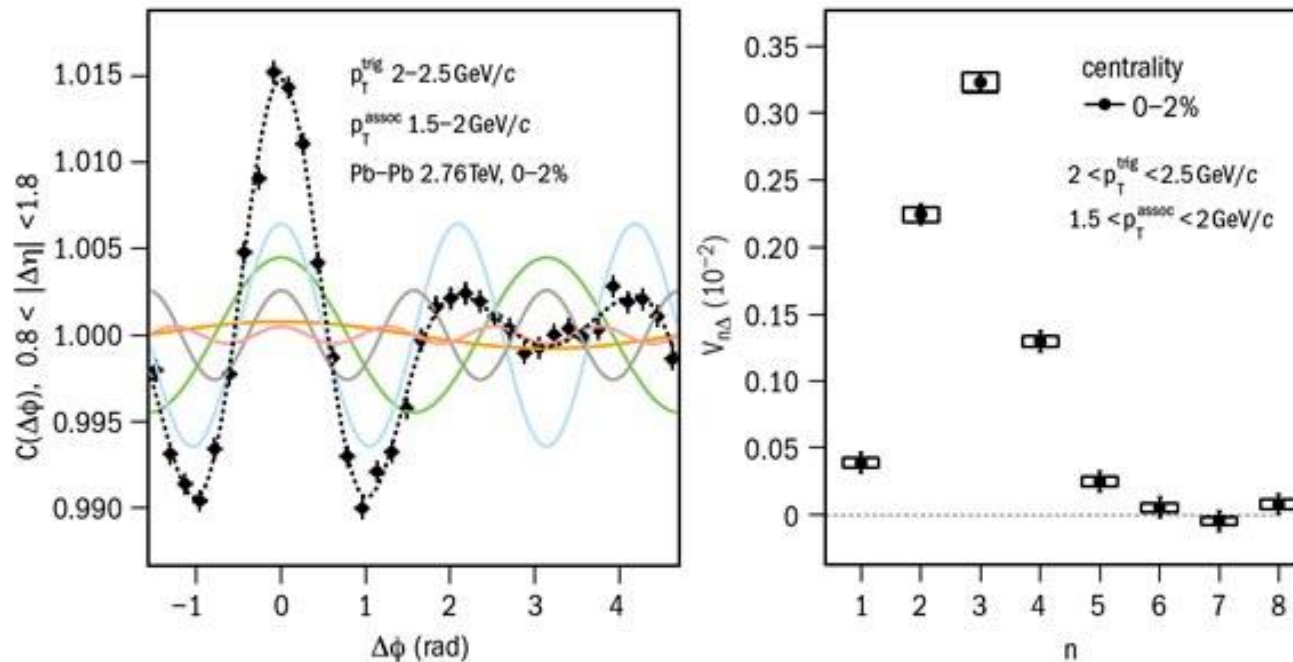
~ spherical with many (16) nearly equal perturbations



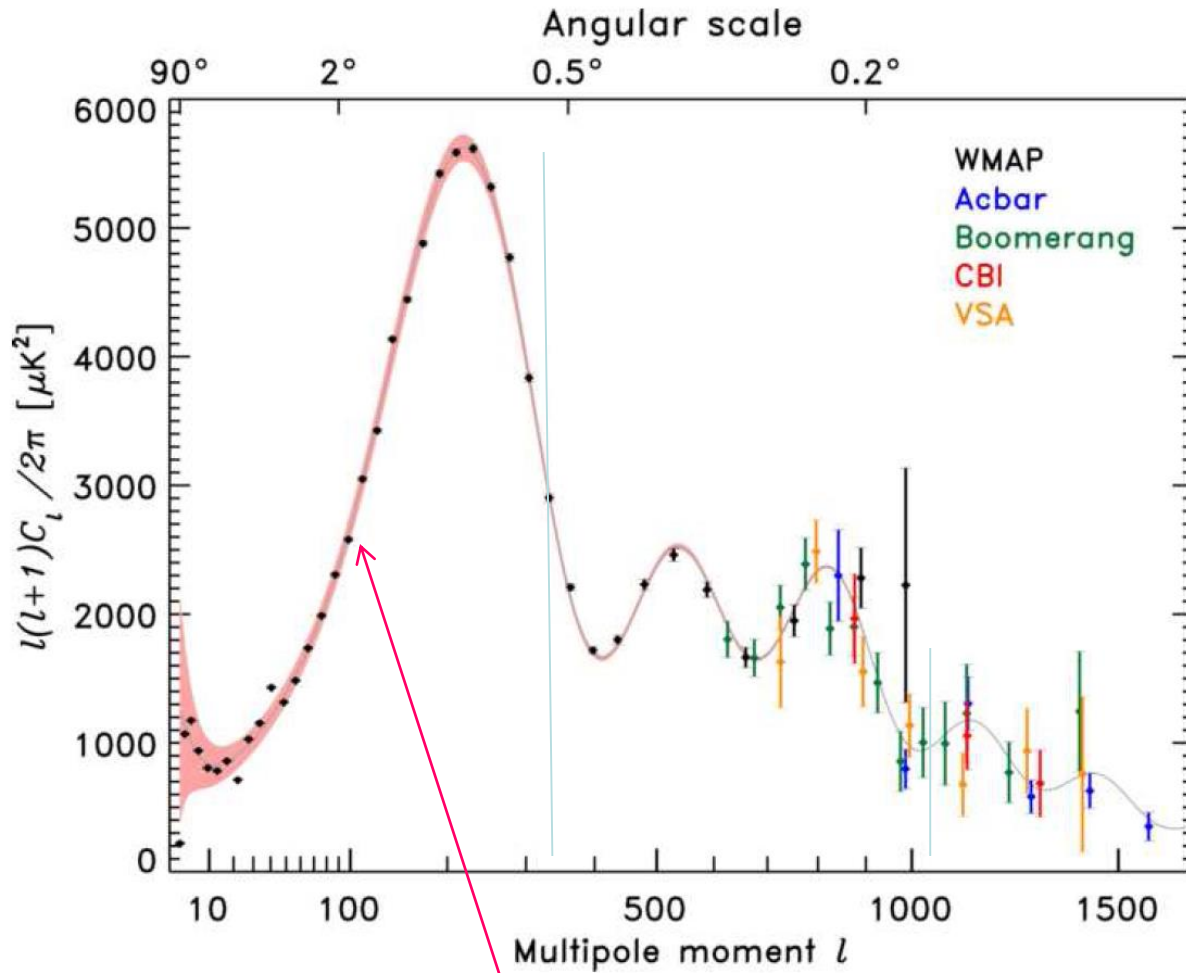
$l = 16$

Sep 23, 2011

ALICE measures the shape of head-on lead-lead collisions



Flow originating from initial state fluctuations is significant and dominant in central and semi-central collisions (where from global symmetry no azimuthal asymmetry could occur, all Collective $v_n = 0$) !



Longer tail on the negative (low l) side !

Fluctuations and polarization, CMB

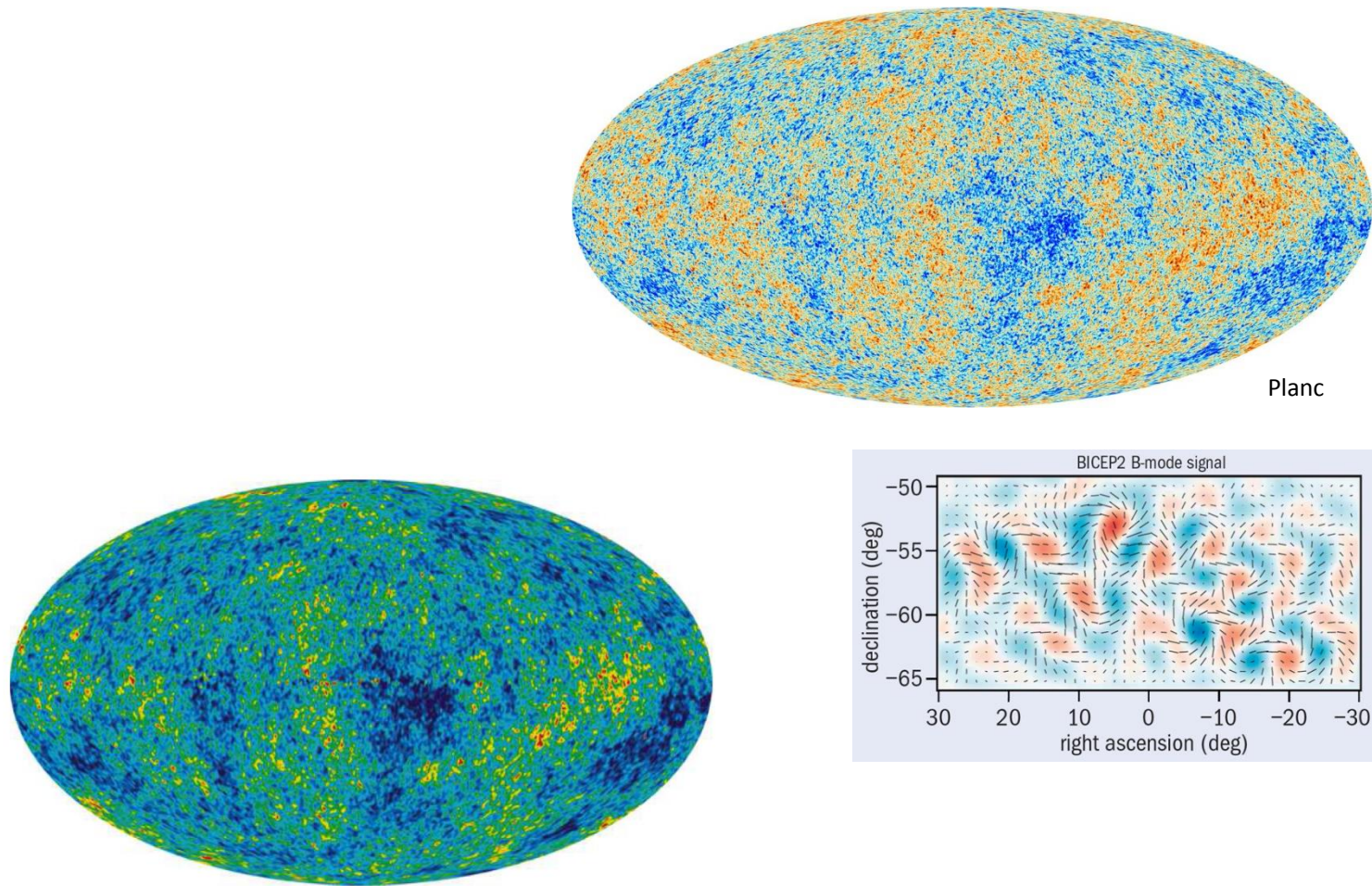
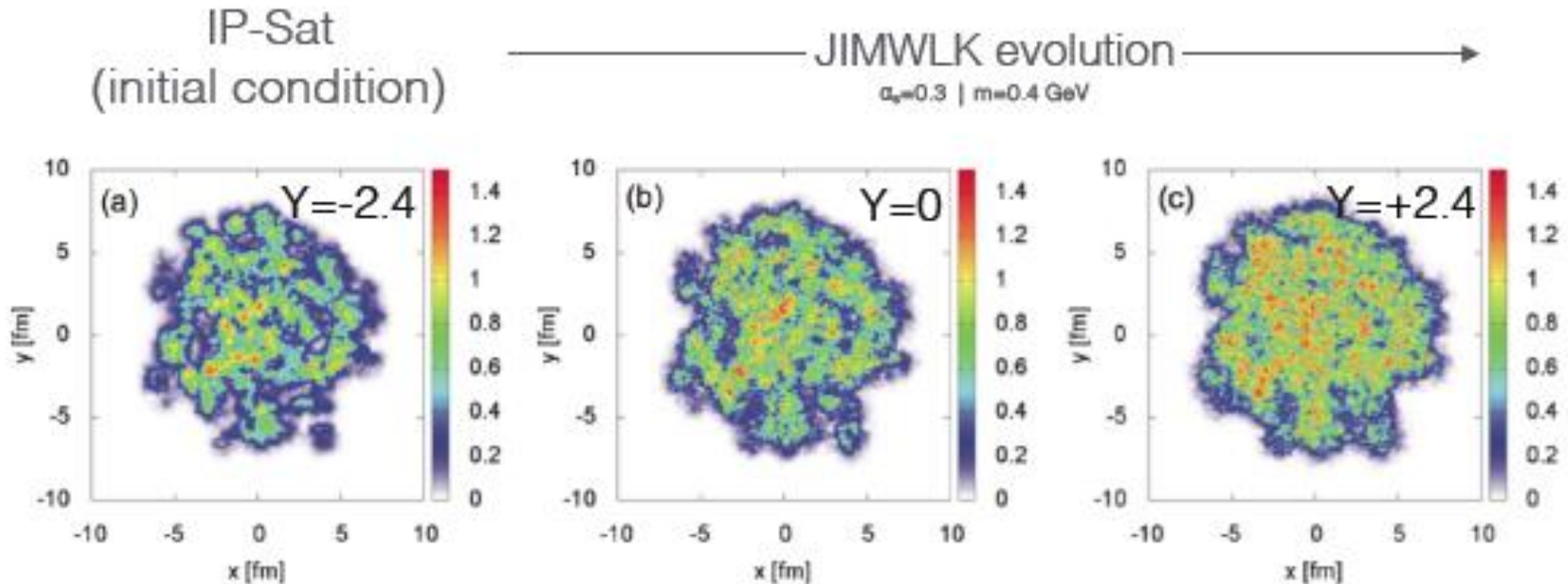


Figure 32: The CMB radiation temperature fluctuations from the 5-year WMAP data seen over the full sky. The average temperature is 2.725K, and the colors represents small temperature fluctuations. Red regions are warmer, and blue colder by about 0.0002 K.

Small-x evolution — results

IS fluctuations in the transverse, $[x,y]$ - plane

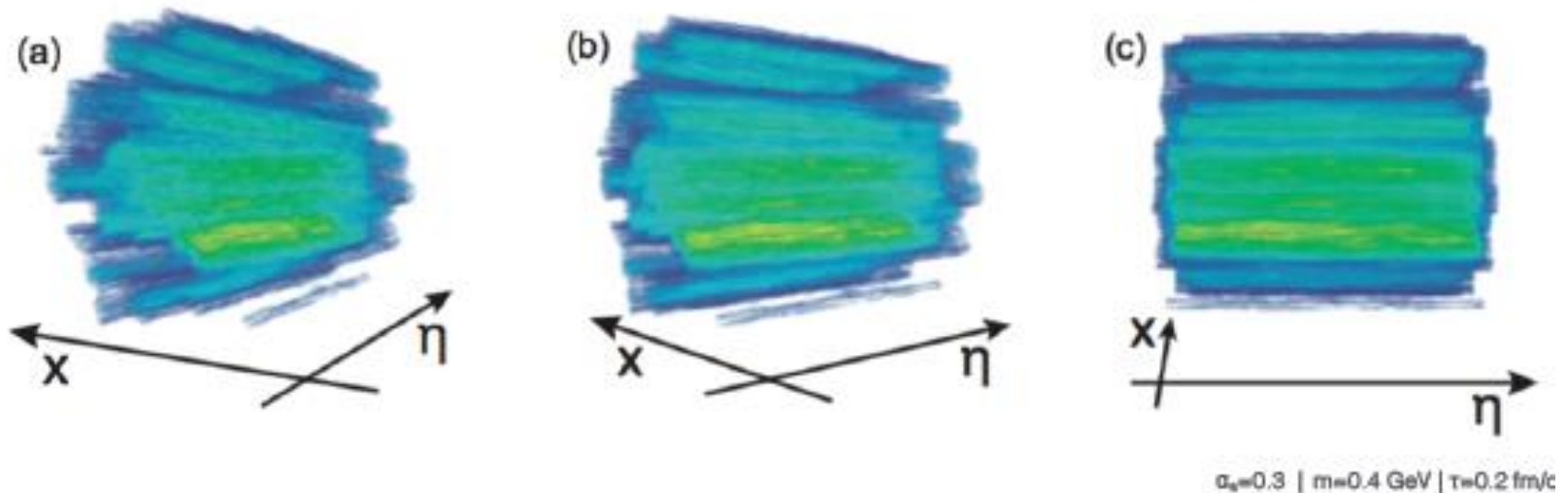


Small scale fluctuations develop and become finer and finer as characterized by the growth of $Q_s(Y)$

Smoothing of geometric profile and growth in impact parameter space ('Gribov diffusion')

3-D Glasma Initial state

Contour plots of initial state energy density ($T^{\tau\tau}$) in a single 2.76 TeV Pb+Pb event ($b=0$)

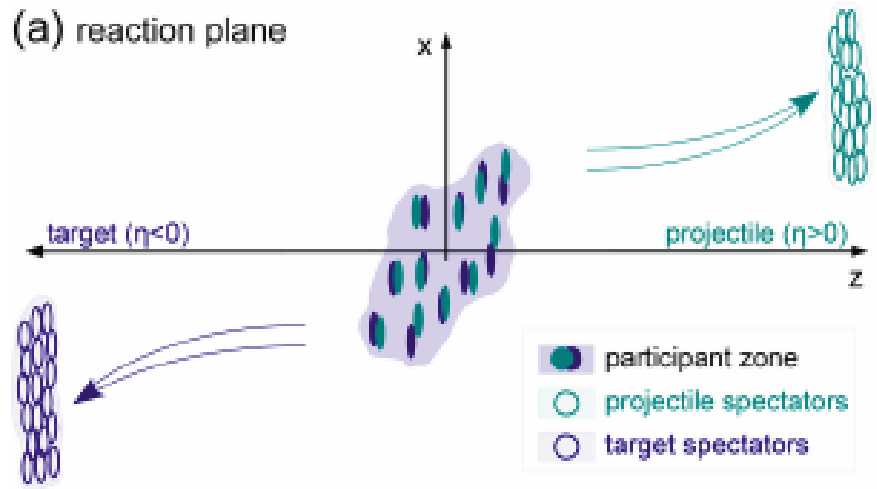
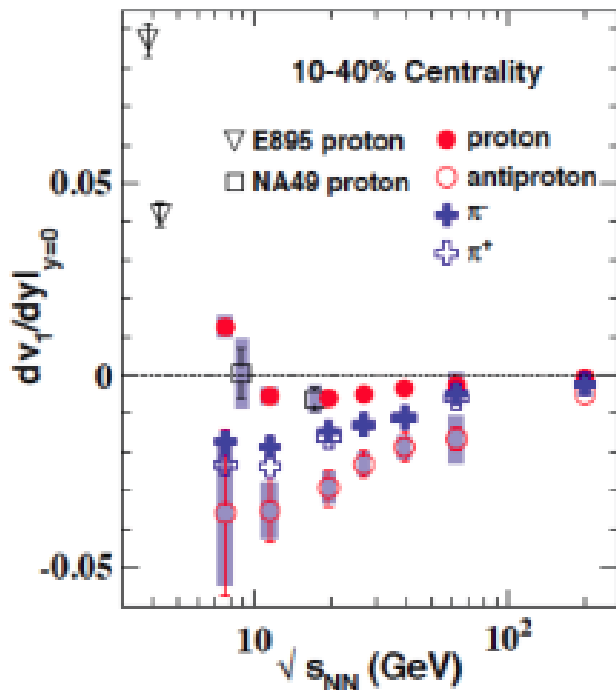


Energy deposition dominated by approx. boost-invariant flux tubes with characteristic transverse size of nucleon

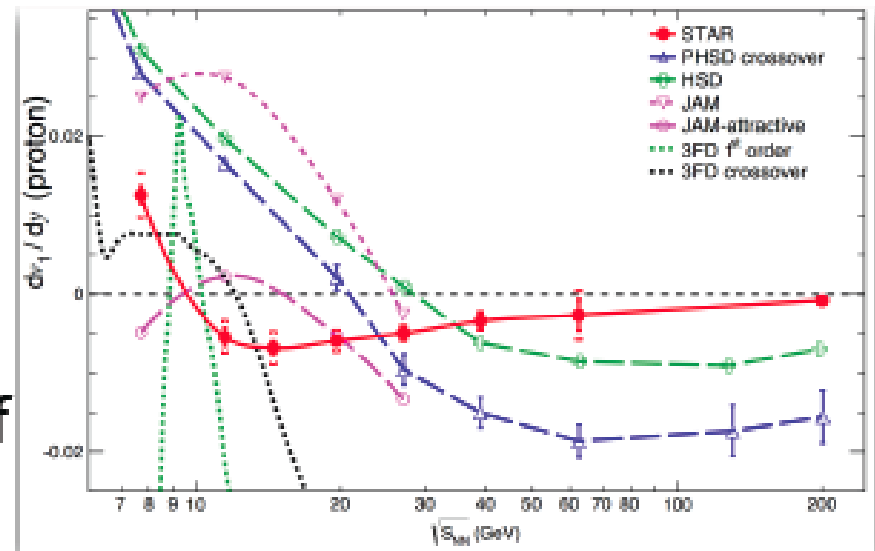
Short & long range fluctuations (η & x), center of mass shifts (η)

Observable #2: Directed Flow

STAR, PRL 112, (2014) 162301



- Non-monotonic energy dependence of v_1 slope
 - First order phase transition?
 - No quantitative agreement of any theory calculation so far



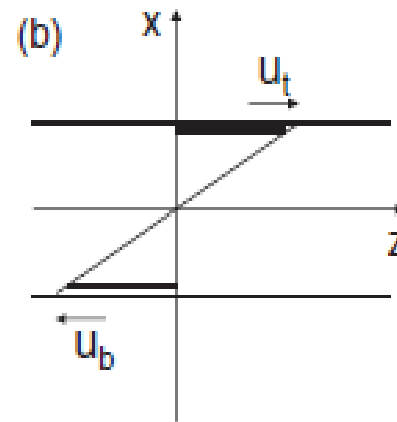
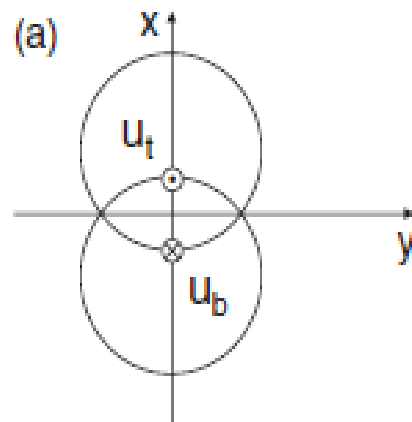
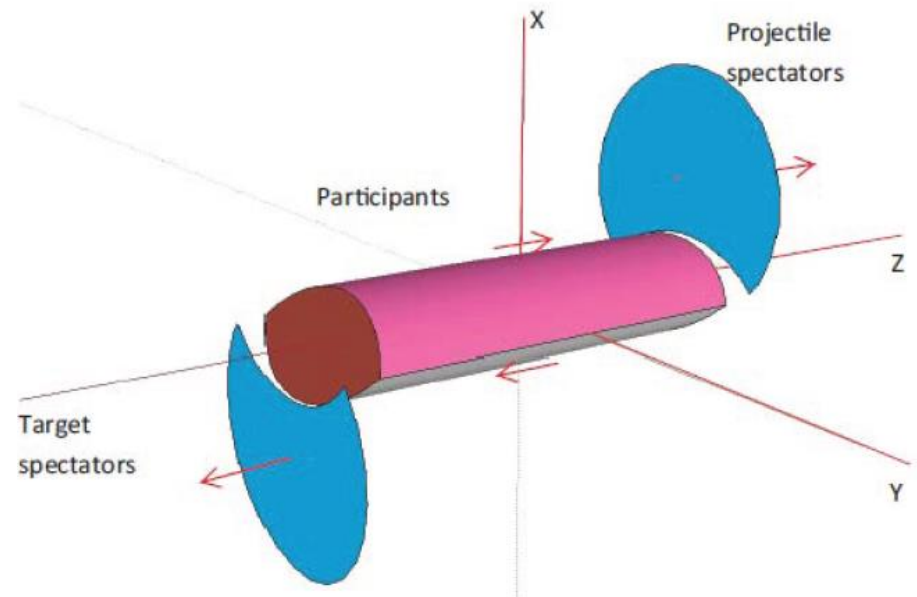
sketch from ALICE, Phys. Rev. Lett. 111

S. Singha, talk at INT-16-3

Break

Peripheral Collisions - Initial State

- Peripheral reactions
- Shear \rightarrow vorticity \rightarrow
- L : in $-y$ direction

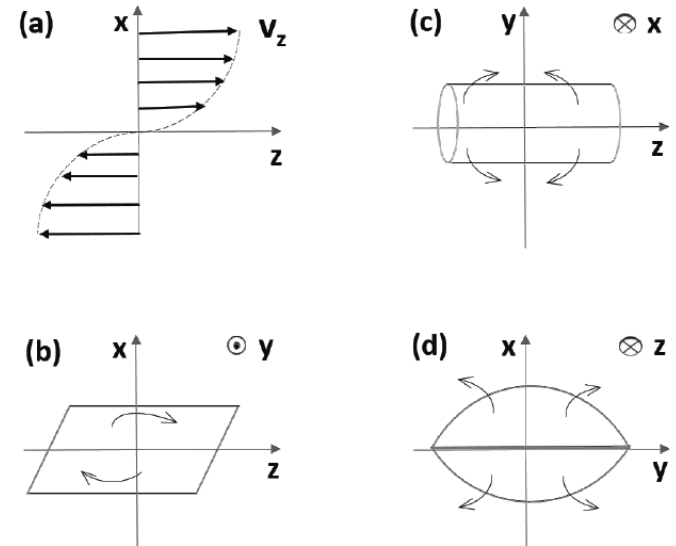
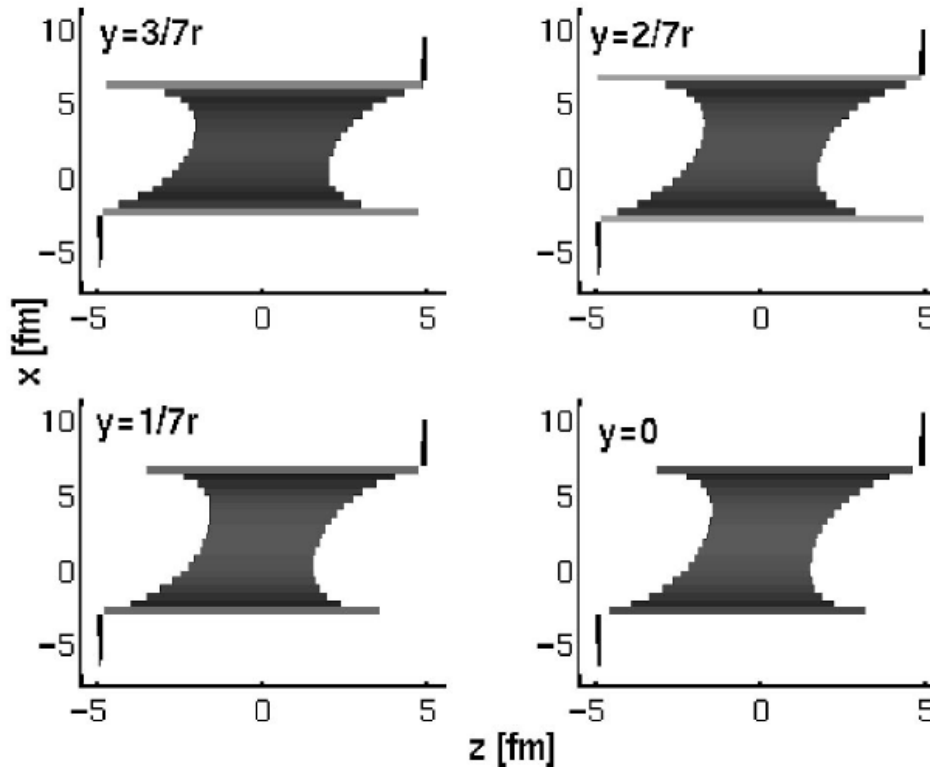
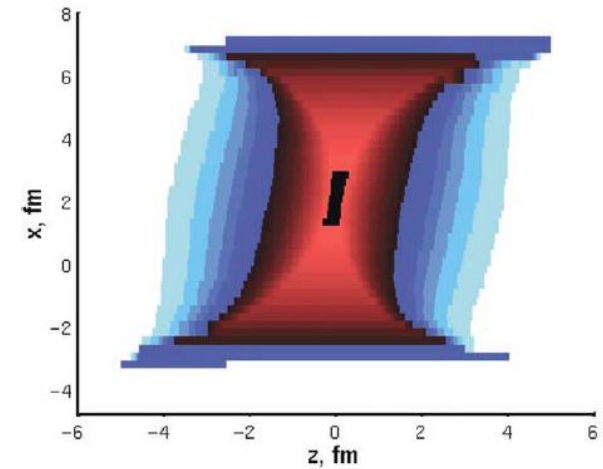


Hw P: $L = ?$

Initial State – Peripheral reactions

Magas, Csernai, Strottman (2001), (2002)

- Yang-Mills flux tube model for longitudinal streaks
- String tension is decreasing at the periphery
- Initial shear & vorticity is present

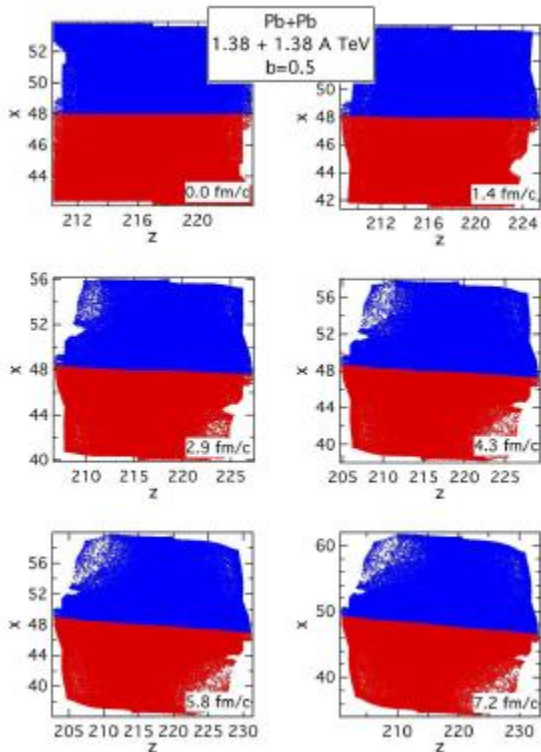


Shear & Turbulence → KHI

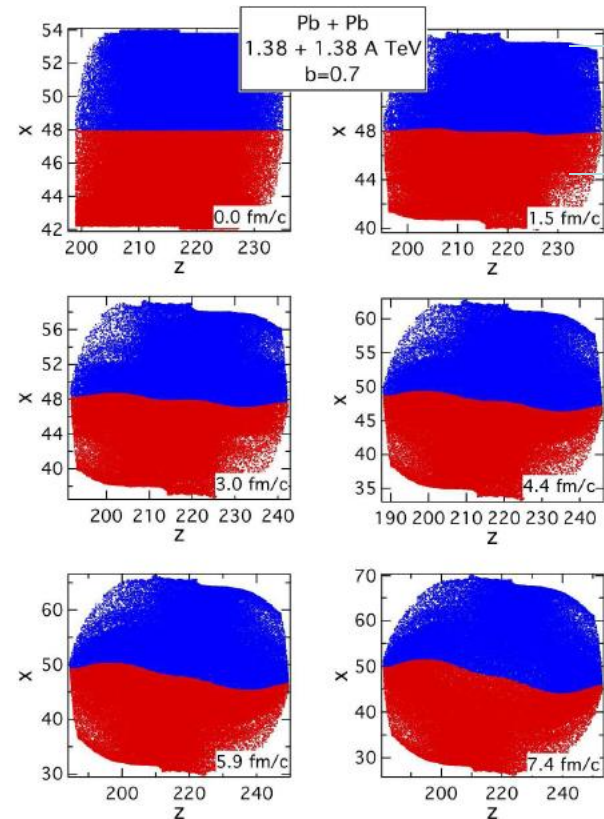
L.P. Csernai^{1,2,3}, D.D. Strottman^{2,3}, and Cs. Anderlik⁴

PHYSICAL REVIEW C **85**, 054901 (2012)

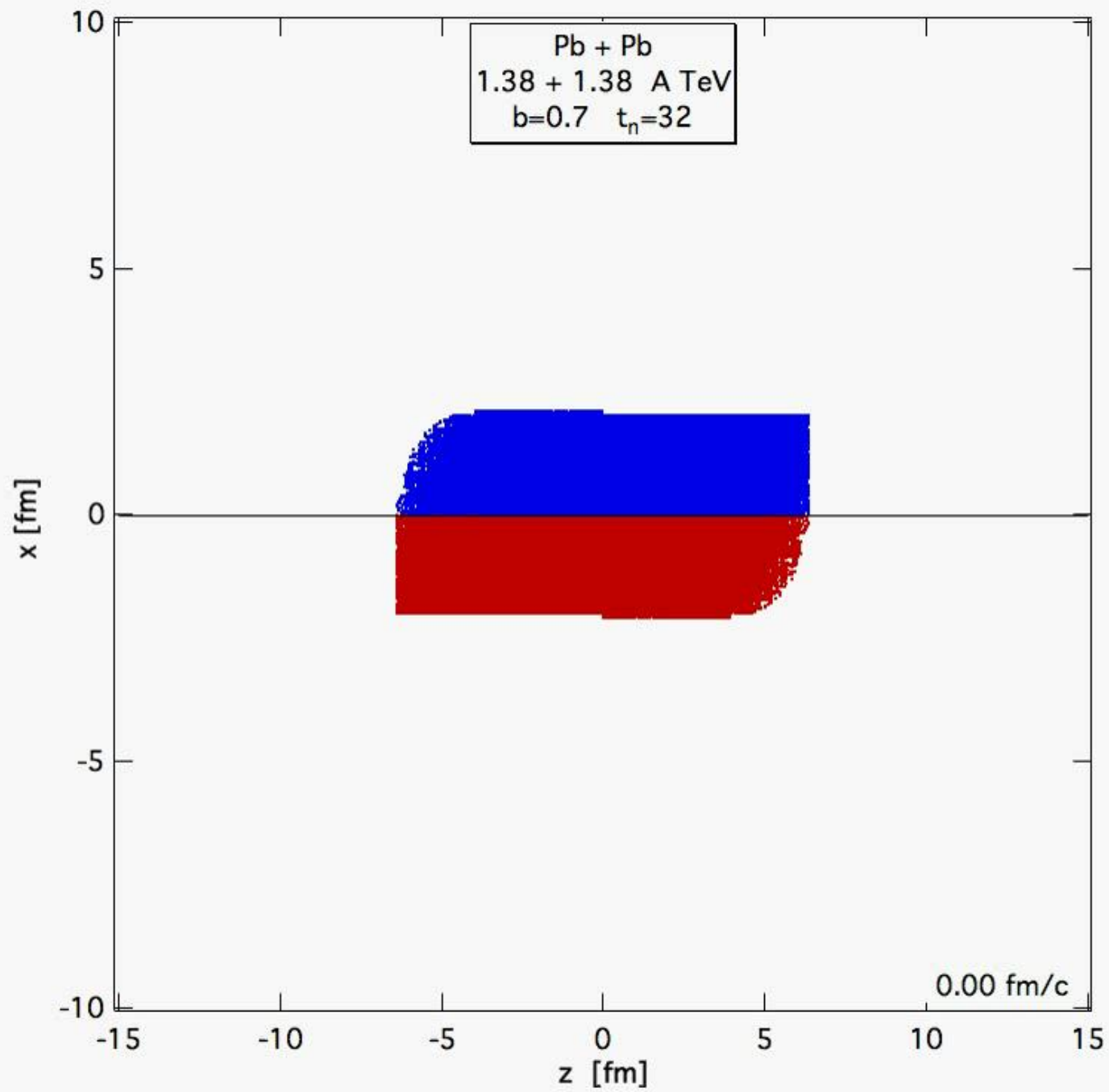
ROTATION – high η



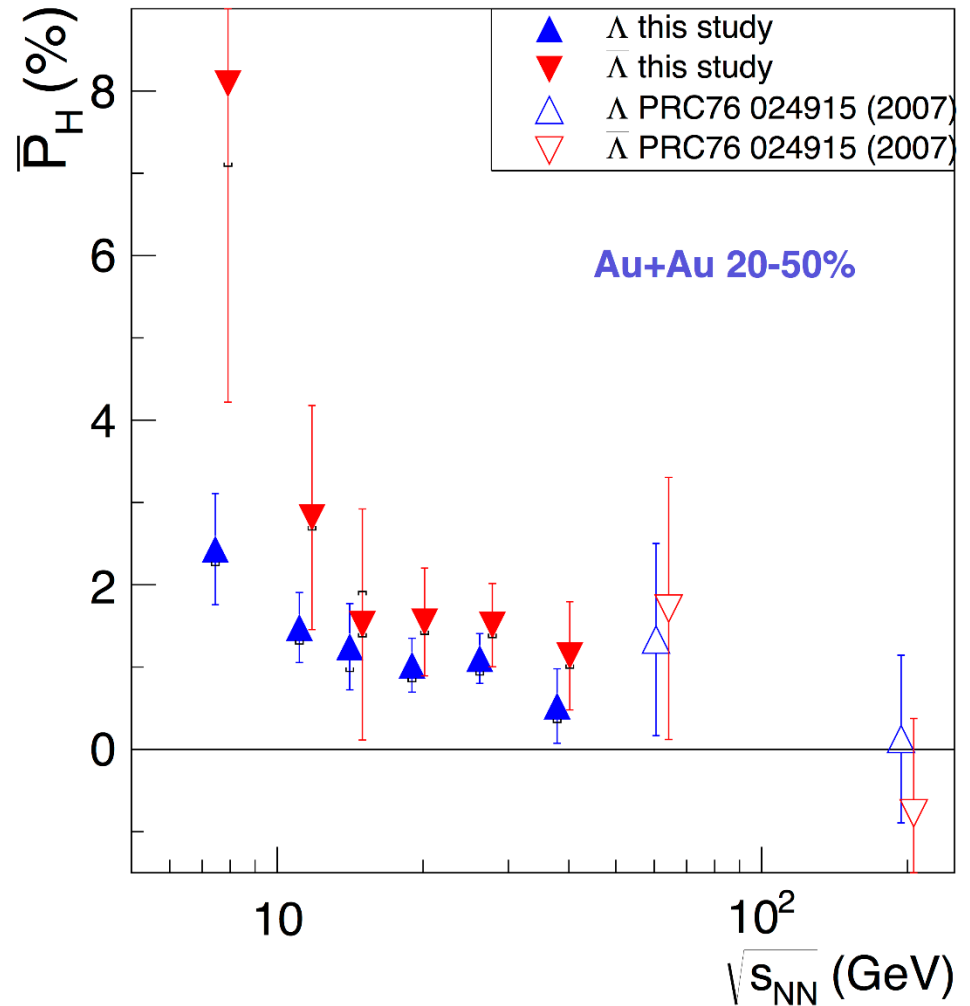
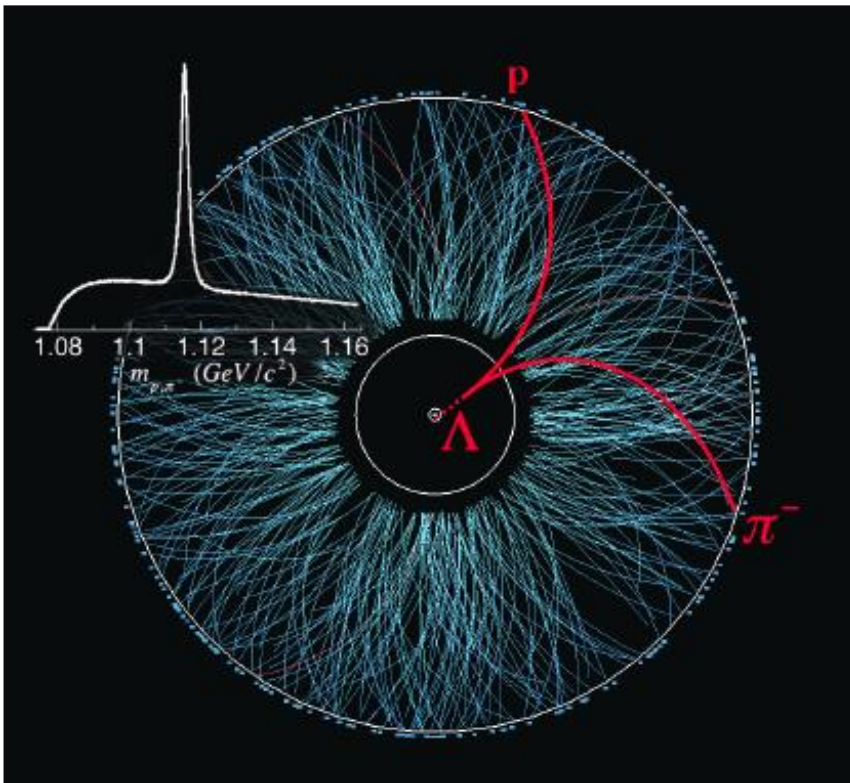
KHI – low η



2.4 fm



Rotation and Turbulence - (2015-16)

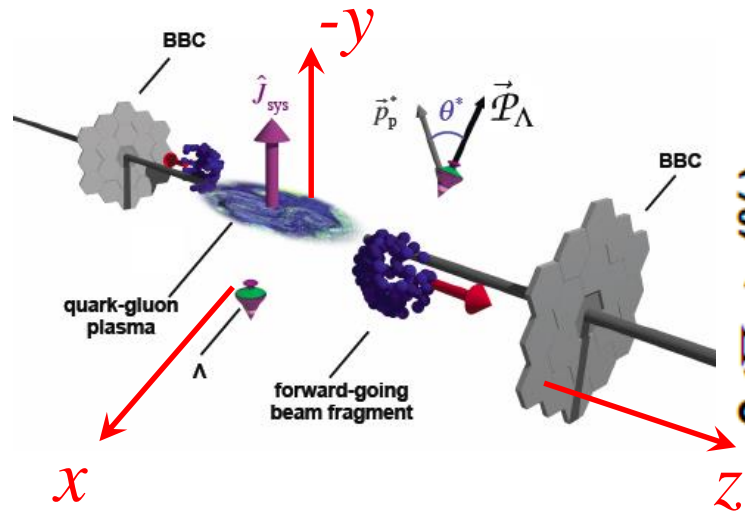


● STAR results

[M.A. Lisa, et al. (STAR Collaboration), Invited talk, QCD Chirality Workshop - UCLA, February 23-26, 2016, Los Angeles, USA. ; QM2017 ; arXiv:1701.06657v1

Observable consequences

[Yilong Xie,¹ Dujuan Wang,² and Laszlo P. Csernai,¹
PHYSICAL REVIEW C **95**, 031901(R) (2017)]



Mike Lisa &
STAR:

Angular mom. →

Vorticity (**rot v**) →

Λ & anti- Λ
polarization

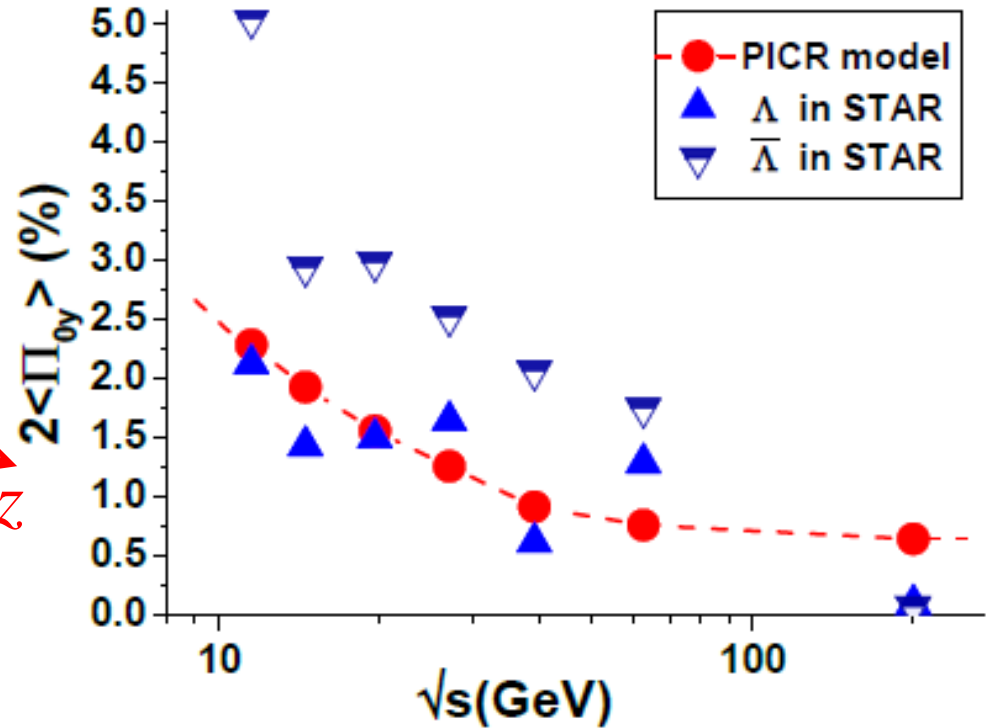


FIG. 4. (Color online) The global polarization, $2\langle\Pi_{0y}\rangle_p$, in our PICR hydro-model (red circle) and STAR BES experiments (green triangle), at energies \sqrt{s} of 11.5GeV, 14.5GeV, 19.6GeV, 27GeV, 39GeV, 62.4GeV, and 200GeV. The experimental data were extracted from Ref[Mike Lisa], dropping the error bars.

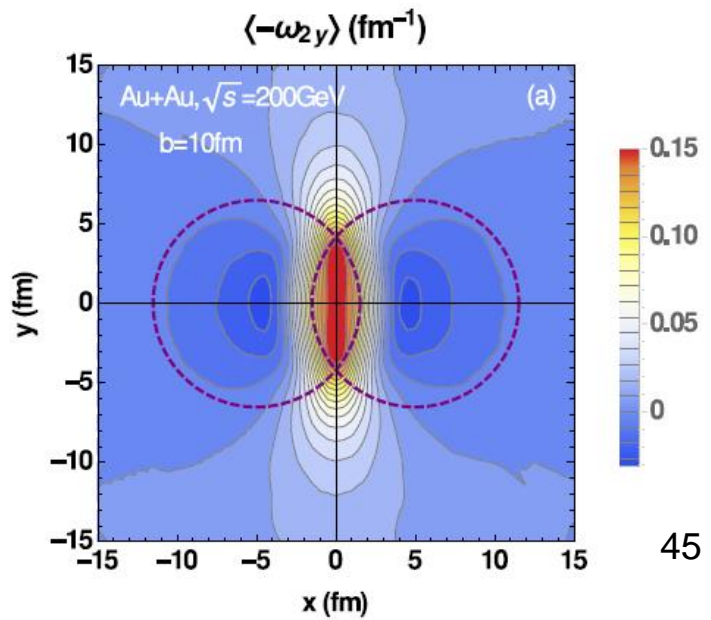
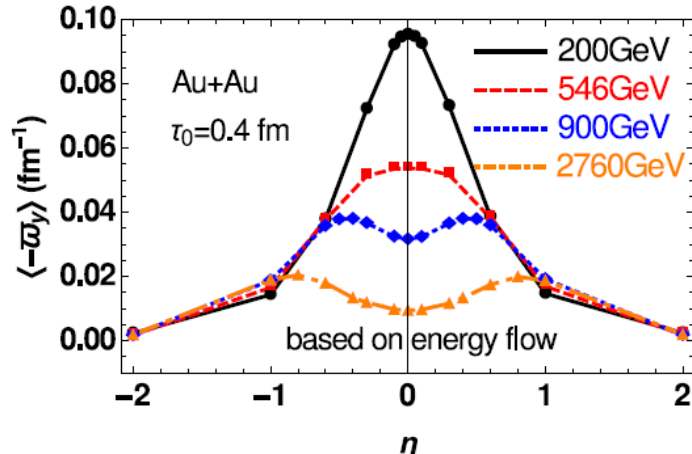
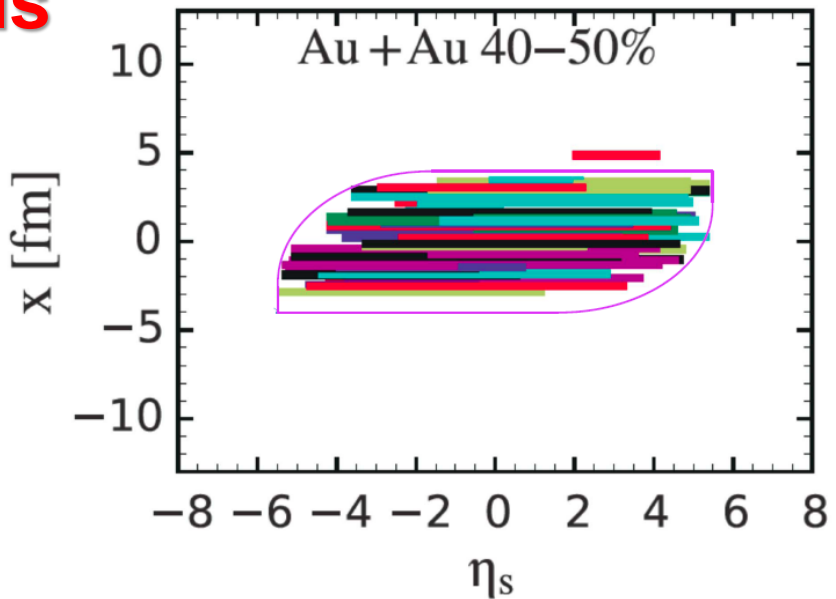
Present parton kinetic models

- **HIJING, AMPT, PACIAE**

Different space-time configurations

[Long-Gang Pang, Hannah Petersen, Guang-You Qin, Victor Roy and Xin-Nian Wang, 27 September - 3 October 2015, Kobe, Japan; and Long-Gang Pang, Hannah Petersen, Guang-You Qin, Victor Roy, Xin-Nian Wang, arXiv: 1511.04131]

[Wei-Tian Deng, and Xu-Guang Huang, arXiv: 1609.01801]

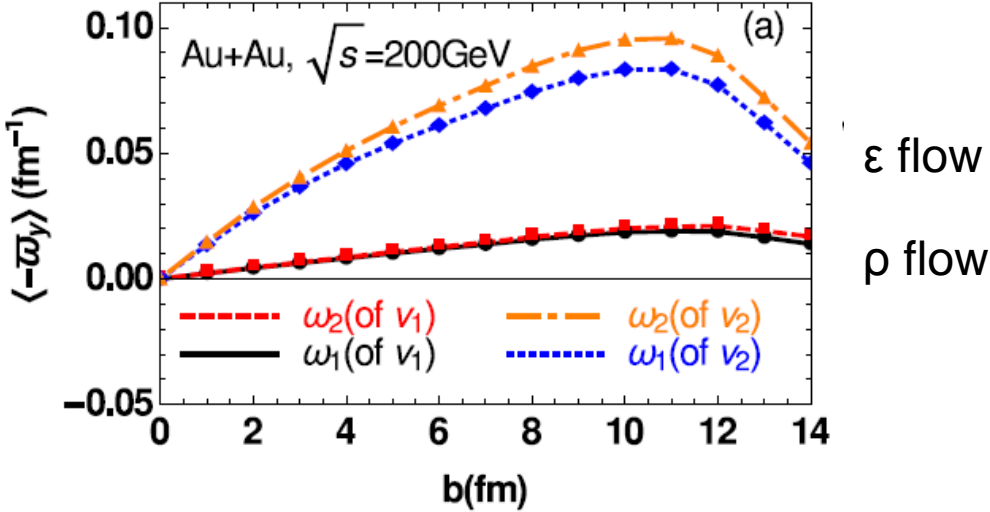
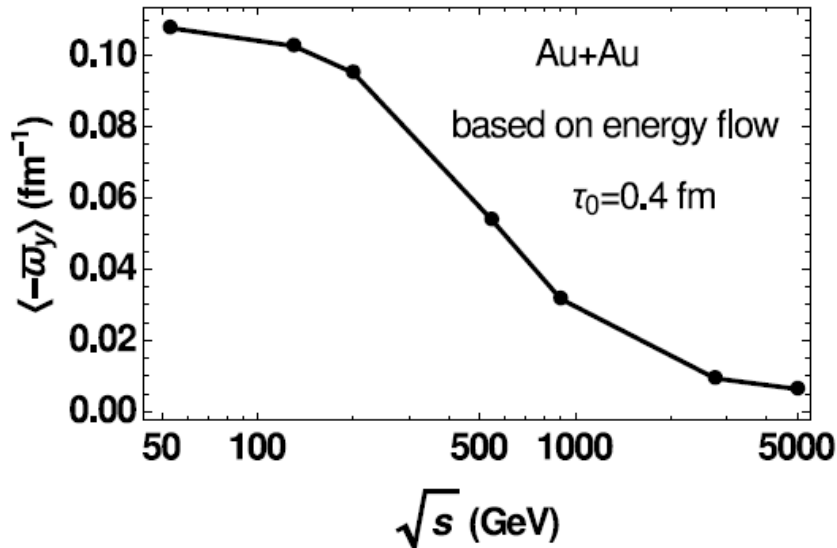
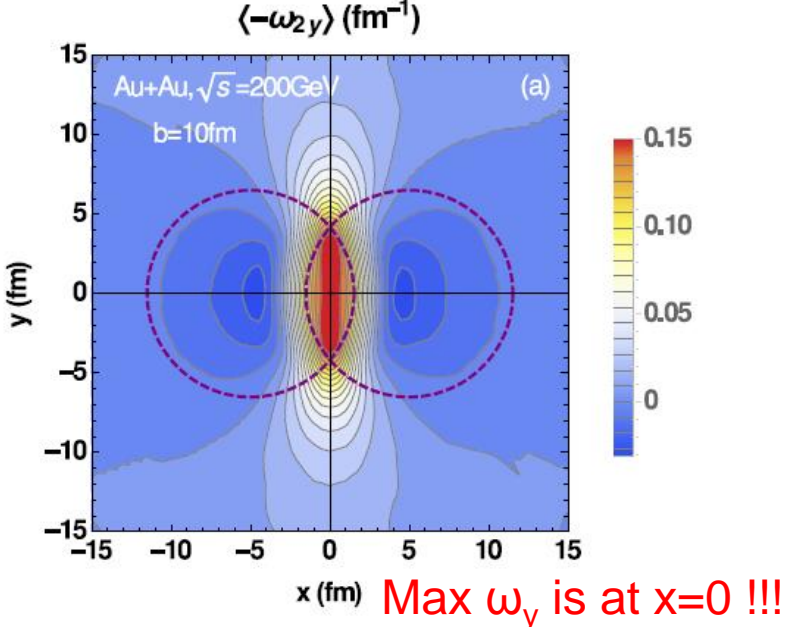


Present parton kinetic models

- HIJING, AMPT, PATHIA

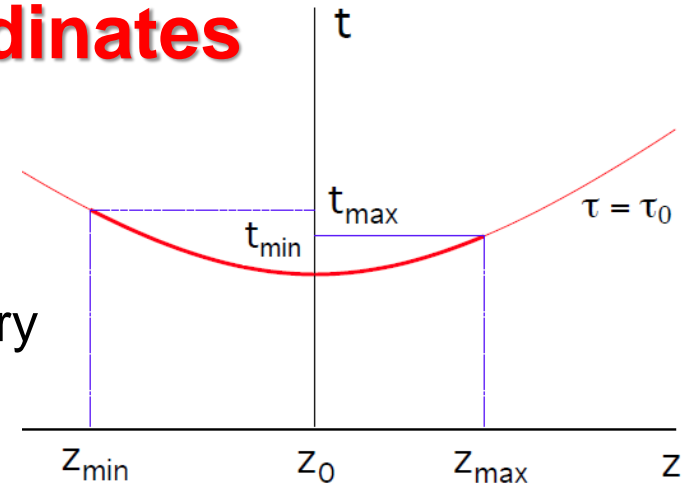
Different space-time configurations

[Wei-Tian Deng, and Xu-Guang Huang, arXiv: 1609.01801]



Initiative: new I.S. in τ, η coordinates

- Separately for each longitudinal streak
- String tension is not decreasing at the periphery
- Initial shear & vorticity is present !



The normal four vector of a hypersurface at $\tau = \text{const.}$ is

$$d\Sigma^\mu = A \tau u^\mu, \quad (3)$$

- Conservation laws: $dN = d\Sigma_\mu N^\mu = \tau A n u_\mu u^\mu d\eta$

$$N_i = N_1 + N_2 = \tau_0 n(\tau_0) A (\eta_{max} - \eta_{min})$$

$$E_i = E_1 + E_2 = \tau_0 e(\tau_0) A (\sinh \eta_{max} - \sinh \eta_{min})$$

$$P_{iz} = P_{1z} - P_{2z} = \tau_0 A e (\cosh \eta_{max} - \cosh \eta_{min}) \quad 47$$

Initiative: new I.S. in τ, η coordinates

- For the i-th streak (t,z) and (τ, η) coordinates are connected as

$$t - t_0 = \tau \cosh \eta ,$$

$$z - z_0 = \tau \sinh \eta ,$$

$$\tau = \sqrt{(t - t_0)^2 - (z - z_0)^2} ,$$

$$\eta = \frac{1}{2} \ln \left(\frac{t - t_0 + z - z_0}{t - t_0 - (z - z_0)} \right)$$

$$= \text{Artanh} \frac{z - z_0}{t - t_0} ,$$

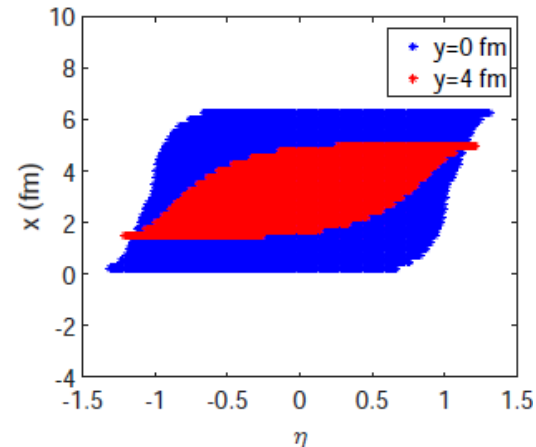
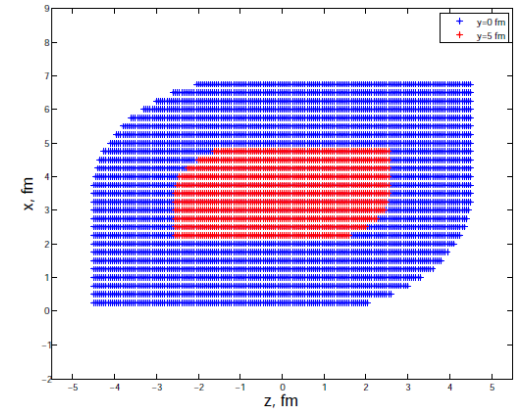
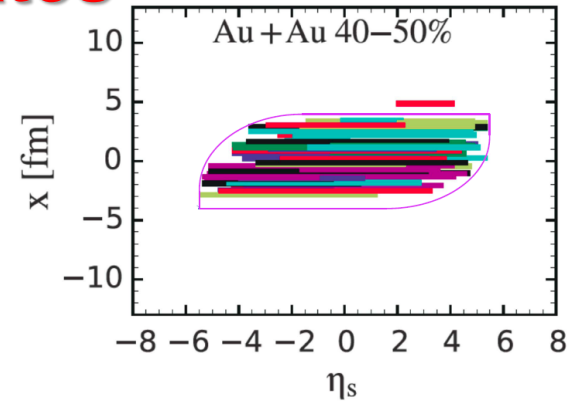
- For the central streak:

$$\frac{1}{2} \Delta \eta_c = \text{arcsinh} \left(\frac{E_c}{2\tau_0 e(\tau_0) A} \right)$$

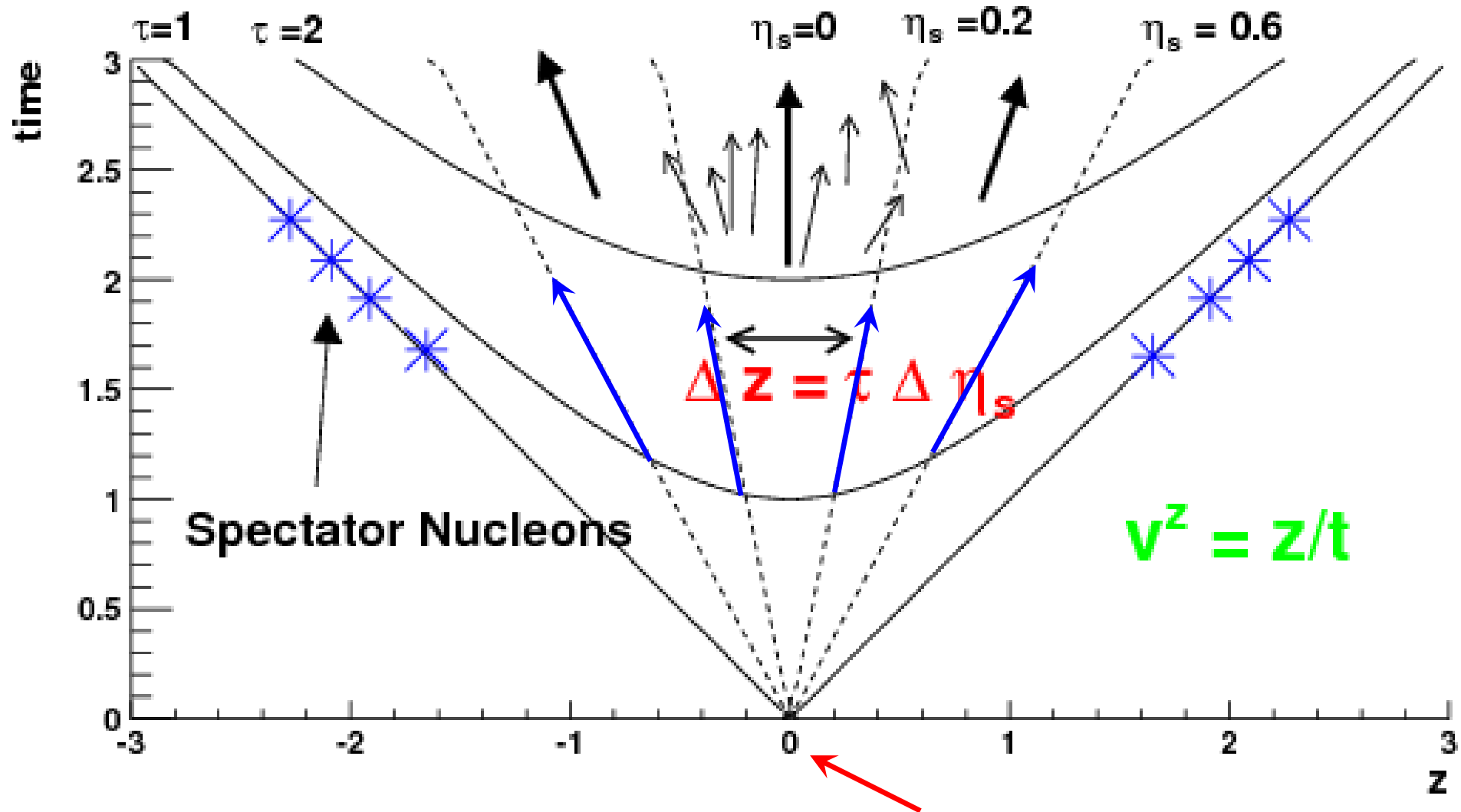
$$z_{c-max} = \tau_0 \sinh \Delta \eta_c ,$$

$$t_{c-max} = \tau_0 \cosh \Delta \eta_c .$$

and



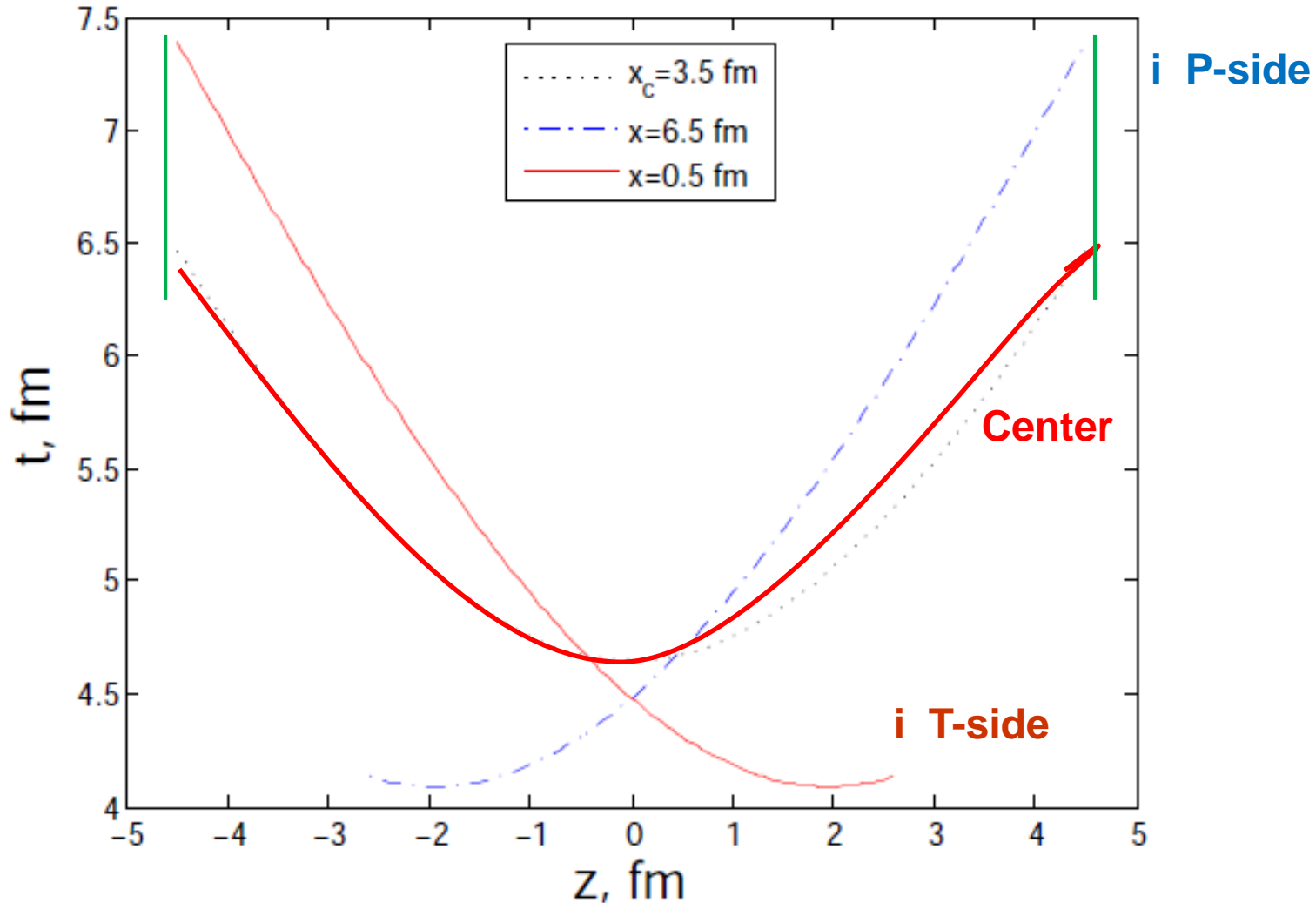
Usual Bjorken model Space-Time structure



All peripheral streaks assumed to have the same origin

Initiative: new I.S. in τ, η coordinates

Thus for each streak, i , we can get the origin of the $\tau=\tau_0$ hyperbola, t_{i0} & z_{i0} .

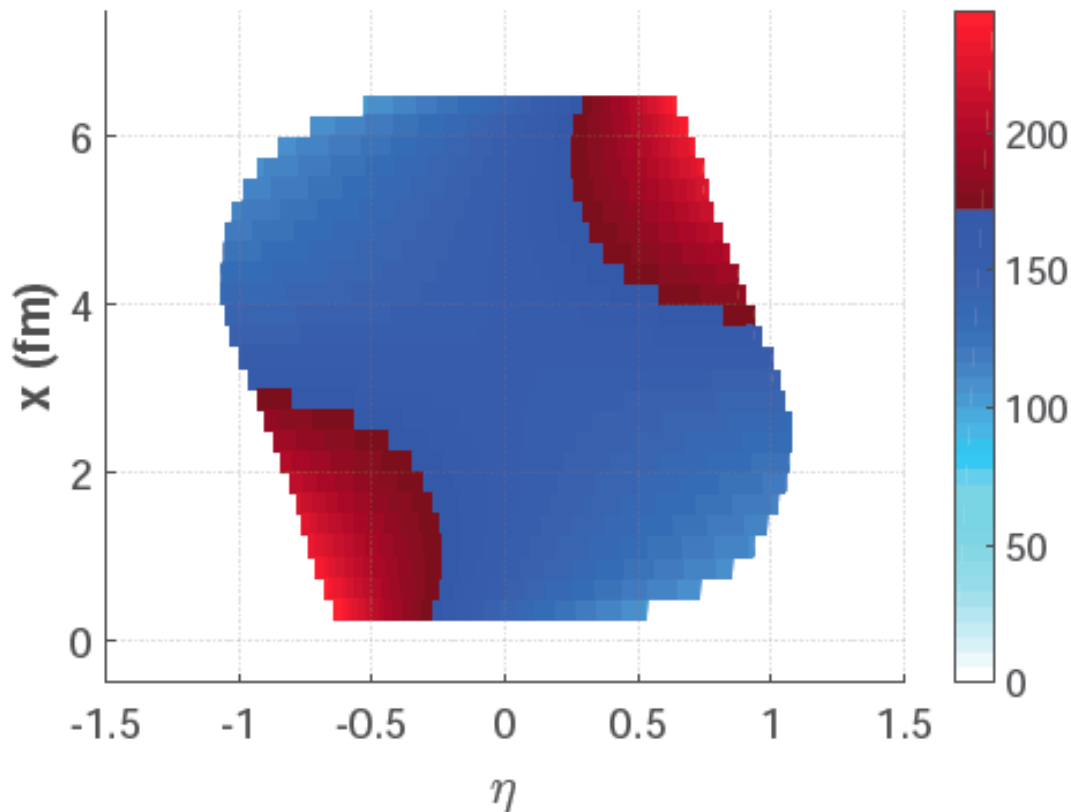


Initiative: new I.S. in τ, η coordinates $\rightarrow x, y, z, t$

Thus for each streak, i , we can get the origin of the $\tau=\tau_0$ hyperbola,

t_{i0} & z_{i0} .

Energy density GeV/fm³



Matching I.S. to hydro

PHYSICAL REVIEW C **81**, 064910 (2010)

Matching stages of heavy-ion collision models,

Yun Cheng, L. P. Csernai, V. K. Magas, B. R. Schlei, and D. Strottman

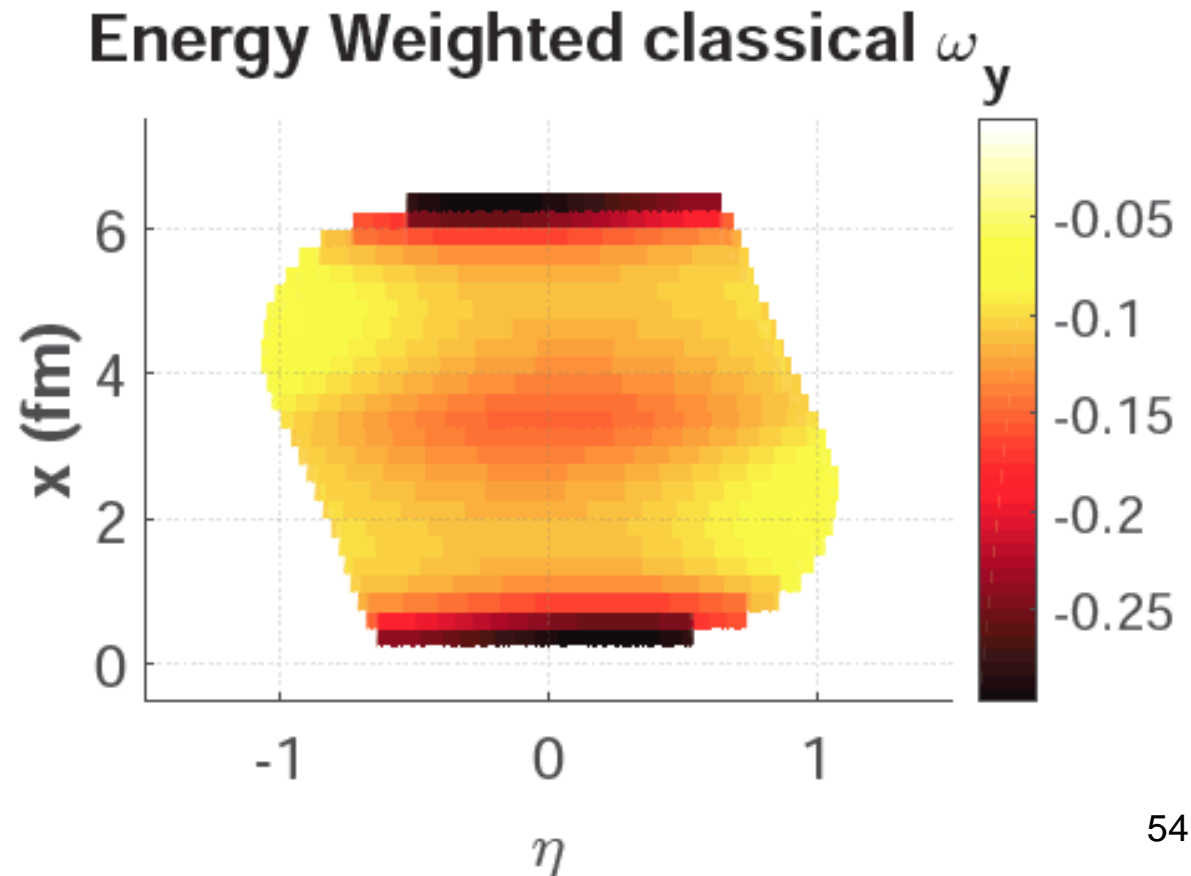
There are hydro options: Cartesian / Bjorken coordinates

Transition surface, $\tau = \text{const.}$, $t = \text{const.}$, curved *h.s.*

In all cases I.S. $T^{\mu\nu} \rightarrow$ Conservation laws due to EoS.

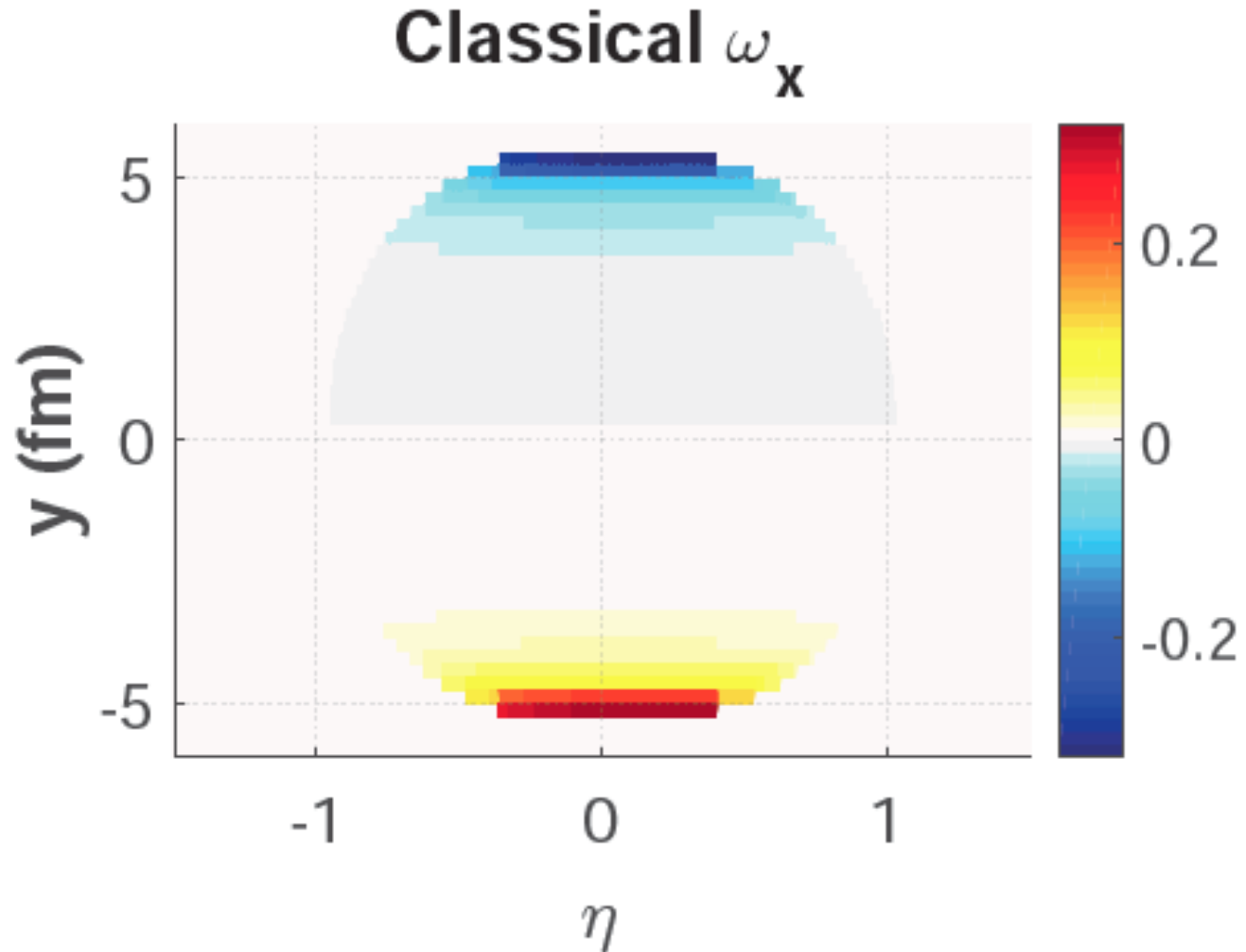
Consequences – vorticity (2017):

- Vorticity is max. at the edges, at high $\pm X$
- Consequence of the Bjorken type model
- Contradicts to AMPT and parton cascade results of [Wei-Tian Deng, and Xu-Guang Huang, arXiv: 1609.01801], where max. is at $x=0$.



Consequences – vorticity (2017):

- Vorticity in x direction is max. at the edges, at high +/- y
- The two edges point to opposite directions, +/- x, i.e. cancel in total ω_x

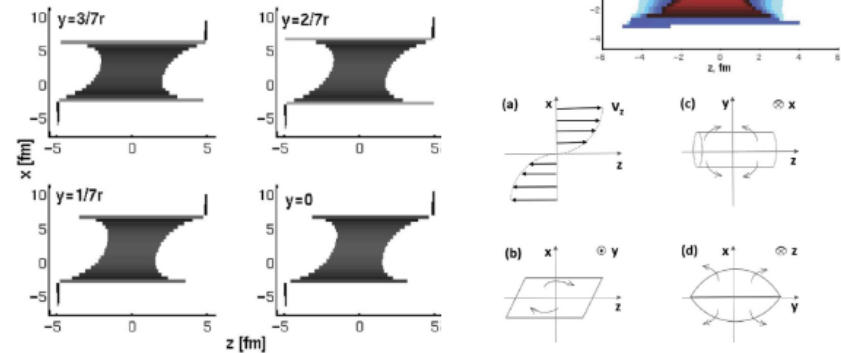


→ Polarization

Initial State – Peripheral reactions

Magas, Csernai, Strottman (2001), (2002)

- Yang-Mills flux tube model for longitudinal streaks
- String tension is decreasing at the periphery
- Initial shear & vorticity is present



With the Yang-Mills streaks initial state
more: Yilong Xie's talk on the boat

Consequences – vorticity (2013):

- Will be similar to the **2001-2** I.S. in (t,z) coordinates
- More compact \rightarrow vorticity may survive better
- The earlier results will remain qualitatively similar:

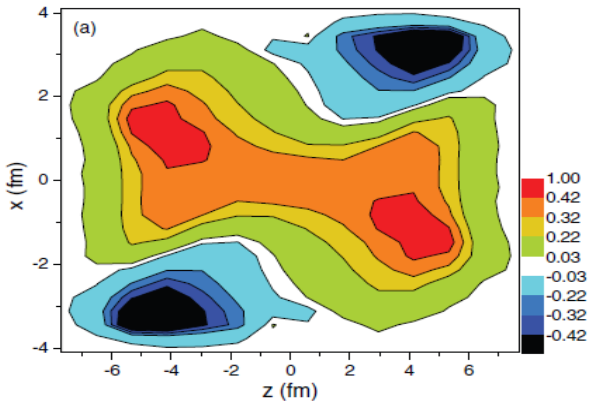
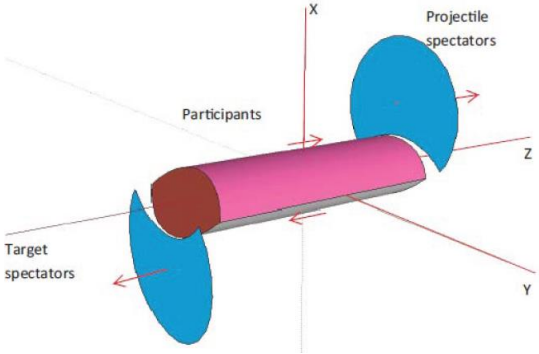


Fig. 3 The vorticity calculated in the reaction (xz) plane at $t = 0.17$ fm/c after the start of fluid dynamical evolution.

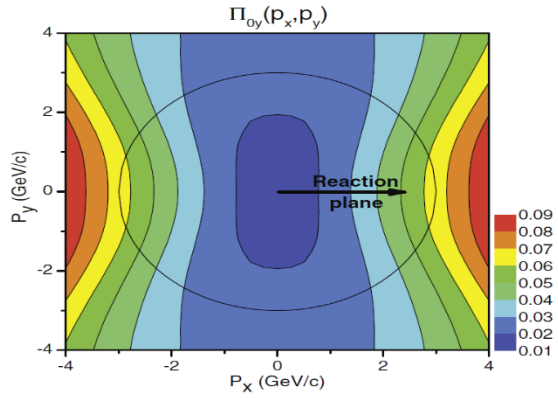


Fig. 4. The dominant y component of the observable polarization, $\Pi_0(\mathbf{p})$ in the Λ 's rest frame.

The initial rotation can lead to observable vorticity (Fig. 3), and polarization (Fig. 4): Leading vorticity term. The initial angular momentum can be transferred to the polarization at final state, via spin-orbit coupling or equipartition.

[L. P. Csernai, et al, PRC **87**, 034906 (2013)]
 [F. Becattini, et al. PRC **88**, 034905 (2013)]

Consequences:

Based on Ref. [Becattini, 2013], Λ polarization can be calculated as:

$$\begin{aligned} \mathbf{\Pi}(p) = & \frac{\hbar\epsilon}{8m} \frac{\int dV n_F(x, p) (\nabla \times \beta)}{\int dV n_F(x, p)} \quad \leftarrow \text{Vorticity, 1st} \\ & + \frac{\hbar p}{8m} \times \frac{\int dV n_F(x, p) (\partial_t \beta + \nabla \beta^0)}{\int dV n_F(x, p)} \quad \leftarrow \text{Expansion, 2nd} \end{aligned}$$

where $\beta^\mu(x) = [1/T(x)]u^\mu(x)$ is the inverse temperature four-vector field. Then thermal vorticity is $\omega = \nabla \times \beta$.

The polarization 3-vector in the rest frame of particle can be found by Lorentz-boosting the above four-vector:

$$\mathbf{\Pi}_0(p) = \mathbf{\Pi}(p) - \frac{p}{p^0(p^0 + m)} \mathbf{\Pi}(p) \cdot p ,$$

[F. Becattini, L.P. Csernai, and D.J. Wang, Phys. Rev. C **88**, 034905 (2013)]

Consequences:

Yilong Xie,¹ Dujuan Wang,² and László P. Csernai¹

Global Λ polarization in high energy collisions

PHYSICAL REVIEW C 95, 031901(R) (2017)

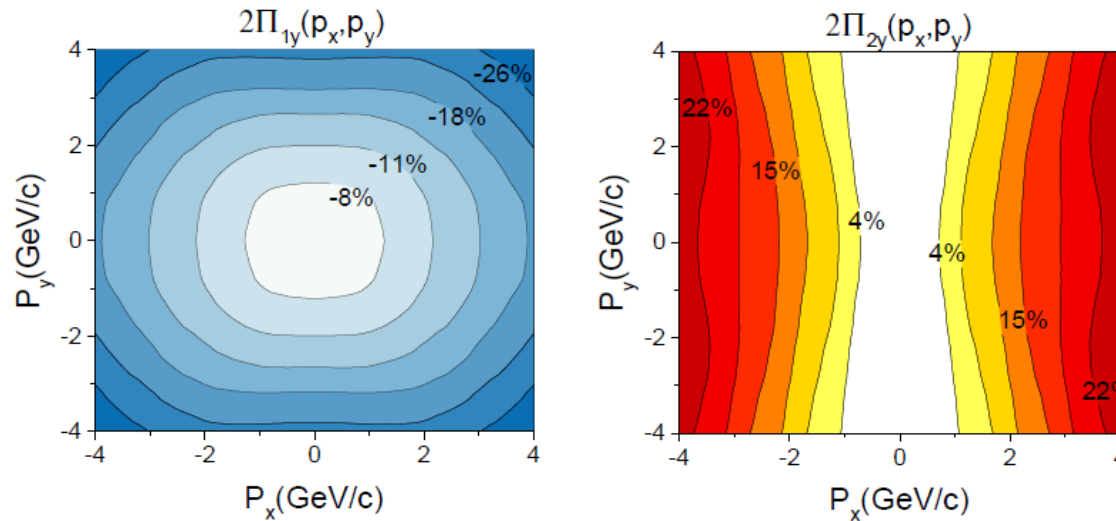
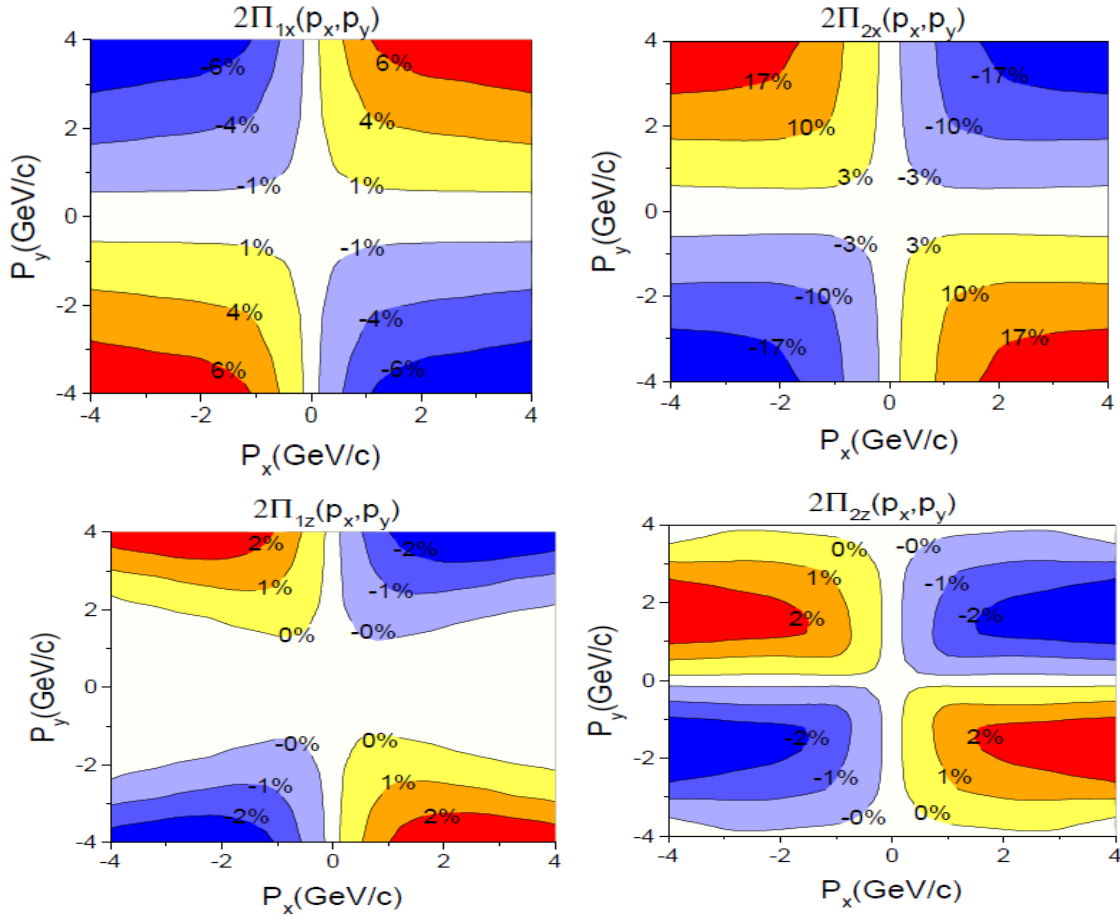


Fig. 6 The first (left) and second (right) term of the dominant y component of the Λ polarization for momentum vectors in the transverse plane at $p_z = 0$, for the FAIR U+U reaction at 8.0 GeV

- The y component is dominant, is up to $\sim 20\%$, as we can compare it with x and z components later.
- 1st & 2nd terms are opposite direction. Result into a relatively smaller value of global polarization.

Consequences

/ c.m. !



1. Anti-symmetry
2. Trivial.

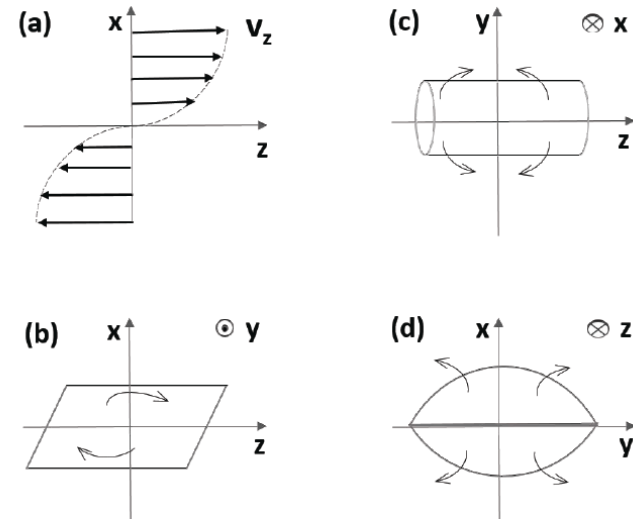
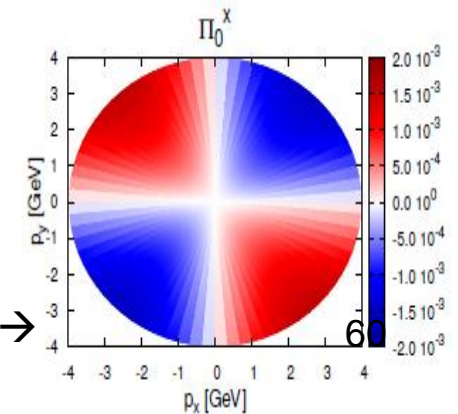
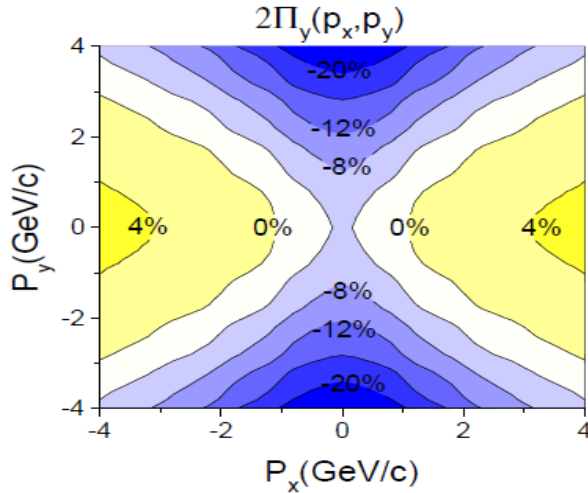


Fig. 7 The first (left) and second (right) terms of the x(up) and y(down) components of the Λ polarization for momentum vectors in the transverse plane at $p_z = 0$, for the FAIR U+U reaction at 8.0 GeV

[Becattini, et al., Eur. Phys. J. C 75, 406 (2015).] →



Consequences FAIR



The modulus of polarization is very similar with the y component of polarization, both in magnitude and the structure. I. e. the other x and z components do not contribute to the polarization, which is in line with previous observations in this work and other papers.

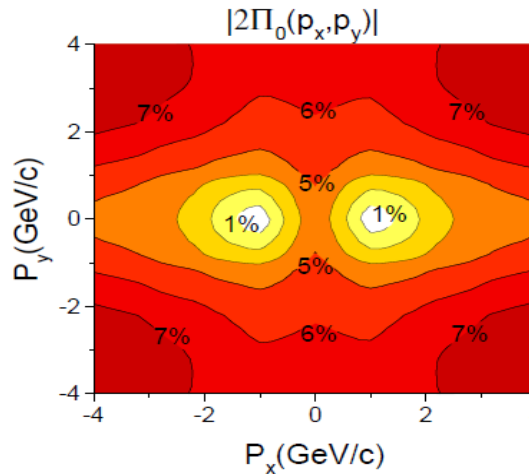
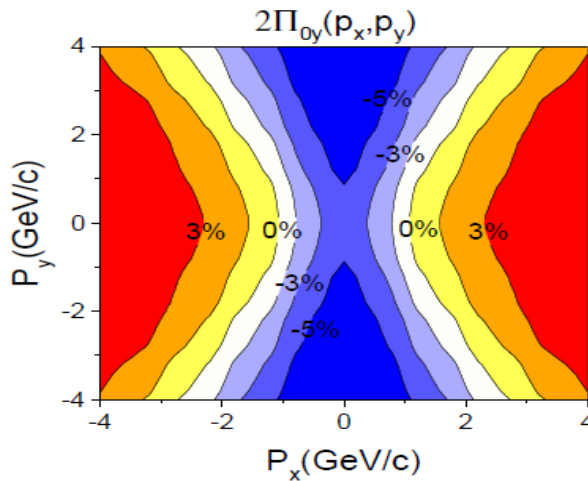


Fig. 8 The y component (left) of polarization vector in center of mass frame and Λ 's rest frame. The right sub-figure are the modulus of the polarization in Λ 's rest frame. At FAIR, 8.0 GeV at time 2.5+4.75 fm/c.

Consequences NICA

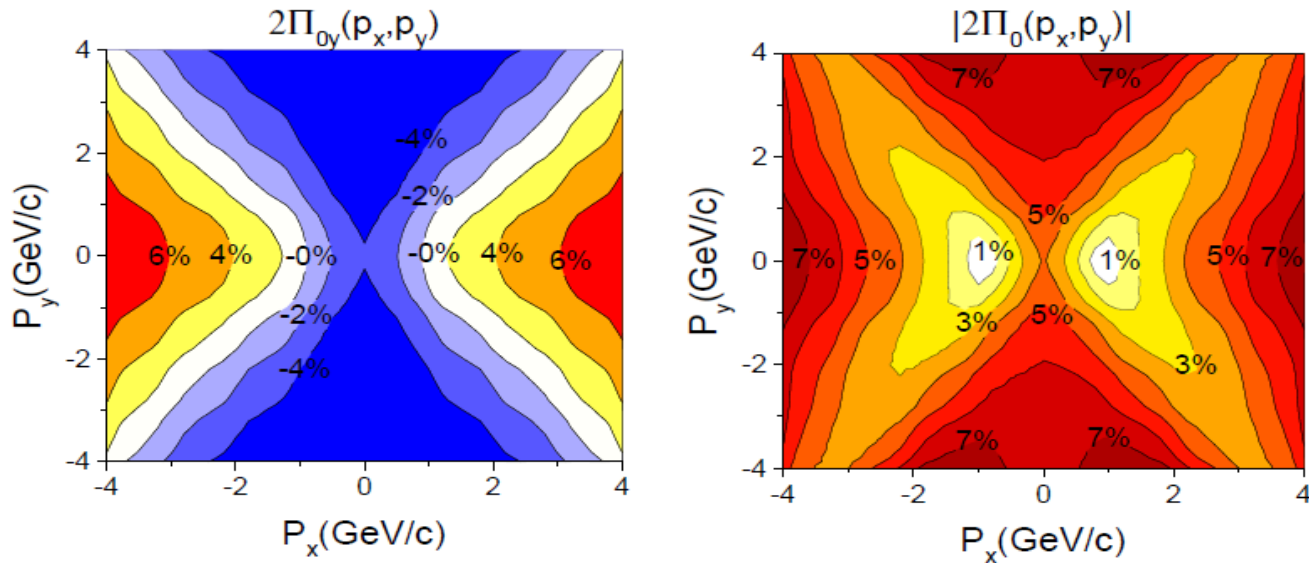


Fig. 9 The y component (left) and the modulus (right) of the polarization for momentum vectors in the transverse plane at $p_z = 0$, for the NICA Au+Au reaction at 9.3 GeV. The figure is in the Λ 's rest frame.

- Similarity between y component and modulus of Polarization, in magnitude and structure.
- Similarity between NICA and FAIR's polarization results.
- The net polarization is still negative, which means the first term is larger than the second term, at this time.

Consequences FAIR

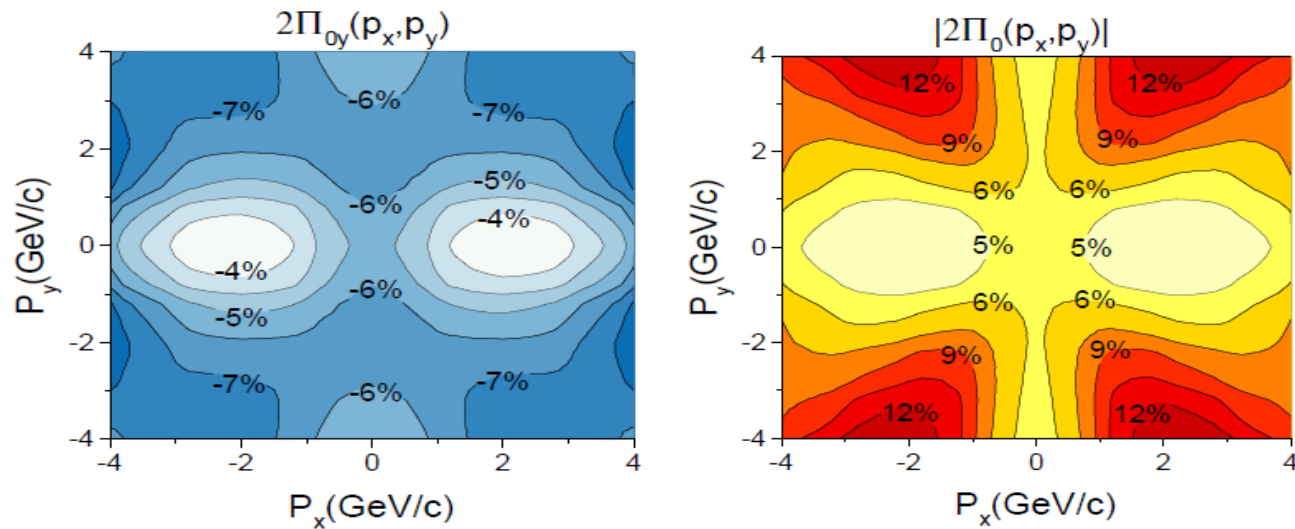


Fig. 9 The y component (left) and the modulus (right) of the polarization for momentum vectors in the transverse plane at $p_z = 0$, for the FAIR U+U reaction at 8.0 GeV, but at an earlier time $t = 2.5 + 1.7 \text{ fm}/c$. The figure is in the Λ 's rest frame.

- Initially, the first term is very dominant

Summary

- Collective flow is the most dominant collective feature of HI reactions.
- Dominant observables change with time, ie v_1 , v_2 , for the EoS and higher harmonics for fluctuations.
- Now peripheral reactions show shear, vorticity (turbulence) for transport coefficients.
- I.S. is of utmost importance, it can be implemented in (t, z) and (τ, η) hydro codes
- Different components, $-y$, x , z , and momentum dependence do show the weight of different dynamical flow patterns.
- → **Highly sensitive diagnostic tools**

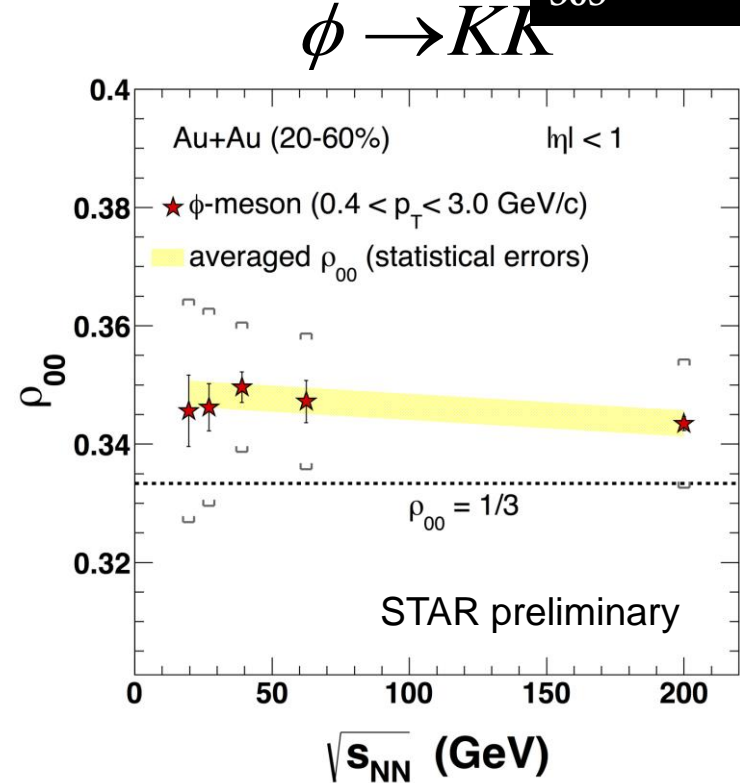
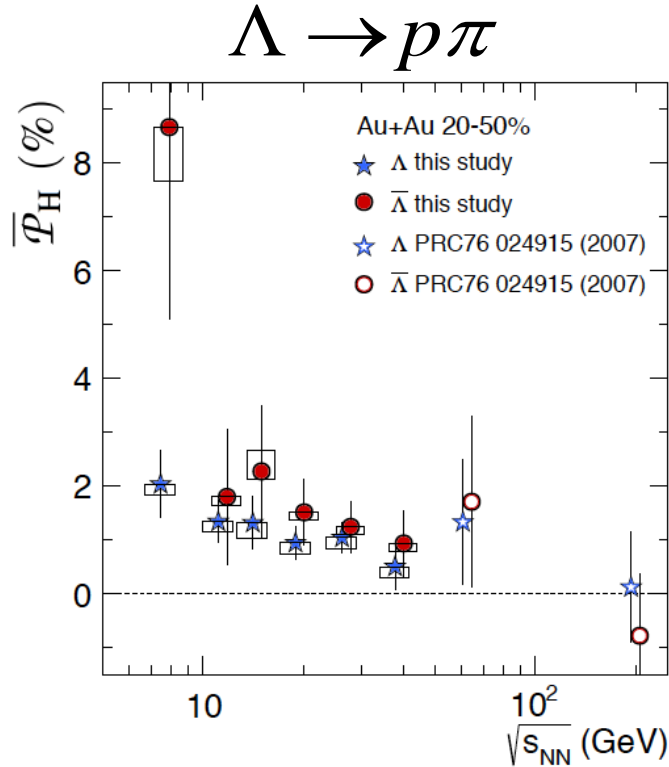
Slides from QM2017 Chicago



Global Λ Polarization and ϕ Spin Alignment

Isaac Upsal, Tue 16:50

Xu Sun, poster 305



- Positive Λ signal \rightarrow positive vorticity
- **First time non-zero signal observed!**
- $\overline{\Lambda} > \Lambda$ (?) \rightarrow magnetic coupling
- First measurement on ϕ meson spin alignment

Λ Submitted

arXiv:1701.06657